Superconductive proximity effect in interacting disordered conductors

M. A. Skvortsov,[1] A. I. Larkin,[1,2] and M. V. Feigel'man[1]
[1]*L. D. Landau Institute for Theoretical Physics, Moscow 117940, Russia*
[2]*Theoretical Physics Institute, University of Minnesota, Minneapolis, Minnesota 55455*
(Received 11 September 2000; published 5 March 2001)

We present a general theory of the superconductive proximity effect in disordered normal-metal–superconducting (N-S) structures, based on the recently developed [M. V. Feigel'man *et al.*, Phys. Rev. B **61**, 12 361 (2000)] Keldysh action approach. In the case of the absence of an interaction in the normal conductor we reproduce known results for the Andreev conductance G_A at an arbitrary relation between the interface resistance R_T and the diffusive resistance R_D. In two-dimensional N-S systems, the electron-electron interaction in the Cooper channel of a normal conductor is shown to strongly affect the value of G_A as well as its dependence on temperature, voltage, and magnetic field. In particular, an unusual maximum of G_A as a function of temperature and/or magnetic field is predicted for some range of parameters R_D and R_T. The Keldysh action approach makes it possible to calculate the full statistics of charge transfer in such structures. As an application of this method, we calculate the noise power of an N-S contact as a function of voltage, temperature, magnetic field, and frequency for arbitrary Cooper repulsion in the normal metal and arbitrary values of the ratio R_D/R_T.

DOI: 10.1103/PhysRevB.63.134507 PACS number(s): 74.40.+k, 74.50.+r, 72.10.Bg

I. INTRODUCTION

The essence of the superconductive proximity effect is the existence of Cooper correlations between electrons in normal metal in contact with a superconductor. The microscopic mechanism leading to the proximity effect is Andreev reflection[2] of an electron into a hole at a normal-metal–superconducting (N-S) interface. The probability of Andreev reflection (as opposed to normal reflection) and thus the strength of the proximity effect is determined by the transparency of the N-S interface, which may be relatively weak due to the presence of a tunnel barrier or mismatch between Fermi velocities of two materials. Disorder in the normal conductor near an N-S contact is shown theoretically[3–6] to increase considerably the effective probability of Andreev reflection (see Ref. 7 for a recent review from the experimental viewpoint). However, when the normal conducting region is made of a dirty metal film or two-dimensional electron gas with low density of electrons, the Coulomb interaction in the normal region (neglected in Refs. 3–6) gets enhanced[8] and leads to strong quantum fluctuations which suppress the Andreev conductance. Several different kinds of quantum effects are known to be relevant in low-dimensional conductors at low temperatures. Quantum corrections to the conductivity of two-dimensional dirty conductors grow logarithmically as temperature T decreases and become large at $\ln(1/T\tau)\sim g$ [where $g=(\hbar/e^2)\sigma$ is the dimensionless conductance, σ is the conductance per square, and τ is the elastic scattering time]. There are two main types of these effects: weak localization corrections,[9,10] and interaction-induced corrections.[8] Other important quantum effects include interaction-induced suppression of the tunneling conductance (Coulomb zero-bias anomaly[8,11]) and disorder-induced suppression[12–16] of the superconductive transition temperature T_c. The corresponding corrections are of the relative order of $g^{-1}\ln^2(1/T\tau)$, i.e., much stronger than the weak localization and interaction corrections.

In the previous paper[1] we have studied the influence of the last two effects on the Andreev conductance and the Josephson proximity coupling in S-I-N and S-I-N-I-S structures (where ''I'' denotes an insulating tunnel barrier). Using the renormalization group method, we have calculated both quantities including the region of strong fluctuations, $\ln^2(1/T\tau)\geqslant g$. Cooper-channel repulsion was found to modify results of semiclassical calculations by the power-law factors $\propto T^{1/\pi\sqrt{g}}$. The effects of the Coulomb zero-bias anomaly (in the case of an unscreened static Coulomb interaction) were found to be even stronger, the corresponding correction factor being of the order of $\exp[-(1/4\pi^2 g)\ln^2(\Delta/T)]$, where Δ is the gap in the superconductive terminal. However, the results of Ref. 1 are limited to the lowest tunneling approximation, i.e., valid under the condition $R_T\gg R_D$, where R_T and R_D are the resistances of the tunnel barrier in the normal state and of the diffusive normal conductor, correspondingly. General semiclassical theory of N-I-S systems with arbitrary ratio R_T/R_D usually neglects interaction effects in the N part of the structure.[3–6] The effect of the Cooper interaction (with strength λ) on the Andreev conductance G_A was studied by Stoof and Nazarov[17] for an N-S structure with the ideal interface and one-dimensional (1D) geometry of the normal wire, in the first order over λ. The relative correction to G_A was found to be small, of the order of $\lambda\ll 1$. The effects of the interaction upon noise in N-S structures had never been studied before, to the best of our knowledge (for a discussion of N-S noise in the absence of an interaction, see Refs. 18 and 19 and the review in Ref. 20).

In this paper we generalize our approach[1] for the case of a strong proximity effect (arbitrary relation between R_T and R_D), in the presence of Cooper interactions in the normal conductor. We calculate the Andreev conductance of 2D N-I-S structures (shown in Fig. 1) at low (compared to Δ) temperature and voltages, as a function of $t=R_D/R_T$ and of

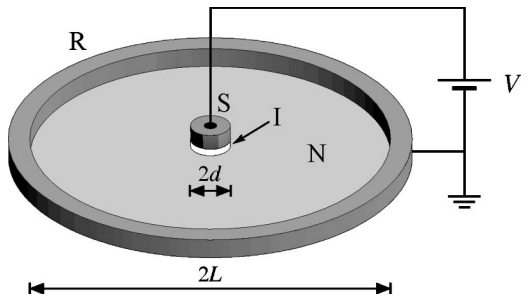

FIG. 1. A small superconductive island (S) of size $2d$ connected to a reservoir (R) through a tunnel barrier (I) and a dirty normal film (N) of size $2L \gg 2d$.

the ''decoherence time'' of an electron and the Andreev-reflected hole, $\hbar/\Omega_*$, where $\Omega_* = \max(T, eV, eDH/c)$. We demonstrate that the Cooper interaction effects in 2D are substantially different from the 1D case considered in Ref. 17. In particular, at $\Omega_* \ll E_{\rm Th} = \hbar D/L^2$ the lowest-order relative correction $\delta G_A/G_A$ scales as $\lambda \ln L/d$ and grows with the size of the system L. We sum up the main logarithmic terms of the order of $(\lambda \ln L/d)^n$ and find that Cooper repulsion may lead to nonmonotonous dependence of G_A on R_D/R_T and/or on the decoherence energy scale Ω_*.

Technically, our method is based on the Keldysh functional approach for disordered superconductors[1] (proposed previously for normal conductors in Ref. 21). The basic object of this theory is the 8×8 matrix field $Q(t,t';\mathbf{r})$ which depends on two time variables and one space coordinate. Its average value gives the electron Green function $G(\mathbf{r},\mathbf{r})$ at coincident points. Fluctuations of the Q matrix describe slow diffuson and Cooperon modes of the electron system. In the case of spin-independent interactions, Q reduces to a 4×4 matrix. This method seems to be more convenient than the replica functional approach[14–16] as it does not require a tedious analytic continuation procedure and allows for the direct study of nonequilibrium phenomena. In the limit $R_T \gg R_D$ studied in Ref. 1, integration over diffuson and Cooperon modes reduces the problem to an effective action $S_{\rm prox}[Q_S, Q_N]$ for the proximity effect, which contains two terms only, $\mathrm{Tr} Q_S Q_N$ and $\mathrm{Tr}(Q_S Q_N)^2$, describing transport of single electrons and Cooper pairs, respectively (here Q_S and Q_N correspond to the superconductive and normal boundaries of the system). At arbitrary relation between R_T and R_D, the proximity action contains an infinite series of terms, $S_{\rm prox}[Q_S, Q_N] \propto \Sigma_{n=1}^{\infty} \gamma_n \mathrm{Tr}(Q_S Q_N)^n$. A set of parameters γ_n can be conveniently parametrized via the 2π-periodic function $u(x) = \Sigma_{n=1}^{\infty} n \gamma_n \sin nx$ that encodes amplitudes of processes of n-electron transfer through the system. The evolution of $u(x)$ as a function of the ratio R_T/R_D is found with the use of the functional renormalization group method applied to the action $S_{\rm prox}[Q_S, Q_N]$.

In this paper we will not consider the weak localization and interaction corrections assuming that the sheet conductance is relatively large, $g \gg \ln(L/d)$. We will also not take into account the effect of the Coulomb zero-bias anomaly (ZBA) on the Andreev conductance. The possibility of neglecting Coulomb ZBA effects while treating the Coulomb-induced repulsion in the Cooper channel[14–16] is due to the fact that the specific form of the Coulomb ZBA depends crucially on the long-range behavior of the Coulomb potential, whereas renormalization of the Cooper-channel interaction depends on the short-distance Coulomb amplitude only. If long-range Coulomb forces are suppressed (i.e., by placing a nearby screening metal gate), the Coulomb ZBA effect may become weak, and the main effect comes from the short-range repulsion in the Cooper channel. This is the situation we are going to study in this paper.

Another limitation of the present discussion is that we will consider the case of a two-dimensional geometry of the current flow between the superconductive and normal electrodes of the structure, as shown in Fig. 1. This will make it possible to construct a unified functional renormalization group treatment that takes into account modifications of the proximity effect strength both due to multiple Andreev reflections and due to Cooper-channel repulsion.

Finally, we restrict our present discussion to a low-frequency domain $\omega \ll D/L^2$. It can be shown that the frequency-dependent Andreev conductance $G_A(\omega)$ does not contain significant frequency dependence at scales $\omega \geqslant D/L^2$, due to the long-range nature of the Coulomb interaction which makes electron liquid effectively incompressible up to a much higher frequency scale defined by the inverse time of electric field propagation across the structure. However, the specific form of the proximity action $S_{\rm prox}[Q_S, Q_N]$ as a linear combination of the traces of $(Q_S Q_N)^n$ is valid only in the low-frequency domain. A general discussion of the action becomes much more involved in the high-frequency region, and we will postpone this subject for future studies.

The rest of the paper is organized as follows. In Sec. II we introduce the Keldysh σ-model action and describe a general scheme of expansion in terms of diffusive slow modes. Section III is devoted to the derivation of the functional renormalization group (FRG) equation for the case of noninteracting electrons in the normal conductor. It is shown that the resulting equation for the function $u(x)$ which parametrizes the action exactly coincides with the Euler equation for the generating function of the transmission eigenvalues T_j discussed in Ref. 22. In Sec. IV we show how physical quantities such as conductivity and current noise can be expressed in terms of the function $u(x)$. The main new results of the paper are presented in Sec. V. In Secs. V A and V B we derive an additional term in the FRG equation, which accounts for the electron-electron interaction in the Cooper channel. The solution of the full FRG equation and the corresponding results for the Andreev conductance are discussed in Sec. V C. The effect of an interaction upon the current noise is studied in Sec. V D. Section VI is devoted to the study of the dependence of the conductance and noise on temperature, voltage, and magnetic field, which suppress the Cooperon amplitude at the energy scale $\Omega_* = \max(T, eV, eDH/c)$. It is shown in Sec. VI C that repulsion in the Cooper channel may lead to a nonmonotonous dependence of the effective interface resistance on Ω_*. Section VII contains a discussion and conclusions. Some technical details are presented in Appendixes A and B. Appendix C contains an analysis of the Andreev conductance in a 2D

S-I-N structure by means of the standard method of the Usadel equation in the presence of a Cooper interaction.

II. KELDYSH σ-MODEL ACTION

The Keldysh action for disordered N-S systems derived in Ref. 1 can be represented as a sum of the bulk and boundary contributions.

The bulk action $S_{\rm bulk}$ is a functional of three fluctuating fields: the matter field $Q(\mathbf{r},t,t')$ in the film, the electromagnetic potential $\vec{\phi}(\mathbf{r},t)$, and the order parameter field $\vec{\Delta}(\mathbf{r},t)$ used to decouple the quartic interaction vertex in the Cooper channel:

$$S_{\rm bulk}=\frac{i\pi\nu}{4}\mathrm{Tr}[D(\nabla Q)^2+4i(i\tau_z\partial_t+\vec{\phi}+\vec{\Delta})Q]$$

$$+\mathrm{Tr}\vec{\phi}^T(V_0^{-1}+2\nu)\sigma_x\vec{\phi}+\frac{2\nu}{\lambda}\mathrm{Tr}\vec{\Delta}^+\sigma_x\vec{\Delta}, \quad (2.1)$$

where D is the diffusion coefficient in the film, ν is the density of states at the Fermi level per single projection of spin, and λ is the dimensionless coupling constant in the Cooper channel.

Being a matrix in the time domain, $Q(\mathbf{r},t,t')$ is also a 4×4 matrix in the direct product $K\otimes N$ of the Keldysh and Nambu spaces. Pauli matrices in the K and N spaces are denoted by σ_i and τ_i, respectively. The field Q satisfies a nonlinear constraint $Q^2=1$ and can be parametrized as $Q=U^{-1}\Lambda U$ where $\Lambda=\Lambda_0\tau_z$ is the metallic saddle point and

$$\Lambda_0(\epsilon)=\begin{pmatrix}1 & 2F(\epsilon)\\ 0 & -1\end{pmatrix}_K. \quad (2.2)$$

The matrix $F(\epsilon)$ introduced in Eq. (2.2) acts in Nambu space and has the meaning of a generalized distribution function. In equilibrium $F(\epsilon)=\tanh(\epsilon/2T)$, and its general form is $F(\epsilon)=f(\epsilon)+f_1(\epsilon)\tau_z$, where $f_1(E)$ is the anomalous distribution function which is a measure of the branch imbalance.[23,24] The object $\vec{\phi}=(\phi_1,\phi_2)^T$ is a vector in Keldysh space, with ϕ_1,ϕ_2 being the classical and quantum components of the field. They are given by the symmetric and antisymmetric linear combination of the ϕ fields on the forward (''f'') and backward (''b'') branches of the Keldysh contour: $\phi_{1,2}=(\phi_{\rm f}\pm\phi_{\rm b})/2$. In the Keldysh technique, external (nonfluatuating) fields (e.g., applied voltage) have only a classical component, while physical results can be obtained by taking derivatives with respect to the quantum component; cf. Sec. IV. Fluctuating fields have both components. $\vec{\phi}$ is a shorthand notation for the matrix $\vec{\phi}=\phi_1\sigma_0+\phi_2\sigma_x$ in Keldysh space. Similarly, $\vec{\Delta}=(\Delta_1,\Delta_2)^T$, and $\hat{\Delta}$ stands for a 4×4 matrix $\hat{\Delta}=[\tau_+\Delta_1-\tau_-\Delta_1^*]\sigma_0+[\tau_+\Delta_2-\tau_-\Delta_2^*]\sigma_x$, where $\tau_\pm\equiv(\tau_x\pm i\tau_y)/2$.

In Eq. (2.1), $V_0(q)$ is the bare static Coulomb potential between electrons in the dirty film. Below we will consider the situation when $V_0(q)$ is screened due to the presence of a nearby metal gate. In particular, if such a gate is situated at a distance b from the dirty film, parallel to it, $V_0(q)=2\pi e^2(1-e^{-2bq})/q\overset{q\to0}{\to}4\pi e^2 b$. As was discussed at length in Ref. 1, the effect of long-range fluctuations of the electromagnetic potential (which lead to the Coulomb zero-bias anomaly) is determined by the long-range part of the bare Coulomb interaction, and thus is suppressed once the Coulomb potential is screened, having the relative order of $g^{-1}\ln(8\pi\nu e^2 b)\ln(1/\Omega\tau)$. We consider the case of a relatively short screening length b, and neglect long-range electric fluctuations and the Coulomb ZBA effects. On the other hand, Coulomb-induced repulsion in the Cooper channel[14,15] does not depend on the long-range part of $V_0(q)$ and is left unchanged by the screening gate. It is this effect of interaction which we are going to consider in this paper.

In terms of the σ model (2.1), diffusionlike collective excitations of an electron system are described as slow fluctuations of the Q matrix over the manifold $Q^2=1$. Small fluctuations near the metallic saddle point $Q=\Lambda$ can be parametrized by the rotation matrix $U=1+W/2+\cdots$, with W obeying the relation $\{W,\Lambda\}=0$. This constraint is resolved by

$$W=u\begin{pmatrix}w_x\tau_x+w_y\tau_y & w_0+w_z\tau_z\\ \overline{w}_0+\overline{w}_z\tau_z & \overline{w}_x\tau_x+\overline{w}_y\tau_y\end{pmatrix}_K u, \quad (2.3)$$

where the matrix u is defined as

$$u=\begin{pmatrix}1 & F\\ 0 & -1\end{pmatrix}_K. \quad (2.4)$$

Variables w_i with $i=0,z$ couple to diagonal in the Nambu space matrices and describe diffuson modes, while w_j with $j=x,y$ couple to off-diagonal in the Nambu space matrices and correspond to Cooperon modes. Their propagators are given by

$$\langle w_i(\mathbf{q})_{\epsilon_1\epsilon_2}\overline{w}_i(-\mathbf{q})_{\epsilon_2\epsilon_1}\rangle=-\frac{1}{\pi\nu}\frac{1}{Dq^2-i(\epsilon_1-\epsilon_2)},$$

$$\langle w_j(\mathbf{q})_{\epsilon_1\epsilon_2}w_j(-\mathbf{q})_{\epsilon_2\epsilon_1}\rangle=-\frac{1}{\pi\nu}\frac{1}{Dq^2-i(\epsilon_1+\epsilon_2)},$$

$$\langle \overline{w}_j(\mathbf{q})_{\epsilon_1\epsilon_2}\overline{w}_j(-\mathbf{q})_{\epsilon_2\epsilon_1}\rangle=-\frac{1}{\pi\nu}\frac{1}{Dq^2+i(\epsilon_1+\epsilon_2)}. \quad (2.5)$$

General contraction rules for averaging of $\langle \mathrm{Tr}AW\cdot\mathrm{Tr}BW\rangle$ over W are listed in Appendix A.

In two dimensions, the action (2.1) can be studied by the renormalization group approach.[15,1] At each step of the RG procedure one has to eliminate fast modes with either $\Omega+\Delta\Omega>\max(Dq^2,\epsilon_1-\epsilon_2)>\Omega$ (for diffusons) or $\Omega+\Delta\Omega>\max(Dq^2,\epsilon_1+\epsilon_2)>\Omega$ (for Cooperons) where Ω is the running ultraviolet RG cutoff. There are two types of logarithmic corrections to the action (2.1). Weak localization and interaction corrections have the relative order of $g^{-1}\ln(1/\Omega\tau)$ and modify the conductance g of the system. Quantum corrections of the other type have the relative order

of $g^{-1}\ln^2(1/\Omega\tau)$ and emerge in renormalization of the Cooper channel coupling λ. They become essential at such scales where localization corrections are still small and can be neglected. In this case λ is the only running parameter of the bulk action which satisfies the RG equation[15,1]

$$\frac{\partial\lambda}{\partial\zeta}=-\lambda^2+\lambda_g^2, \quad \lambda_g=\frac{1}{2\pi\sqrt{g}}, \tag{2.6}$$

where $\zeta=\ln(1/\Omega\tau)$ is the logarithmic variable. The first term on the right-hand side (RHS) of the RG equation (2.6) is due to the usual BCS logarithm, whereas the second contribution is the effect of Coulomb repulsion between slowly diffusing electrons.

The bulk action (2.1) describes dynamics of the electron system in the metal film. The possibility of tunneling between the island and the film is taken into account in the lowest tunneling Hamiltonian approximation by introducing the boundary term in the action:

$$S_{\rm tun}=-\frac{i\pi\gamma}{4}{\rm Tr}_\Gamma Q_{\rm isl}Q. \tag{2.7}$$

Here $Q_{\rm isl}$ refers to the island, spatial integration under the trace is taken over the area of the interface Γ, and γ is the dimensionless normal-state tunneling conductance per unit area of the boundary.

Below we will consider thick enough superconductive island so that the absolute value $|\Delta|$ of the order parameter is not suppressed by proximity to the normal film. The corresponding condition reads $|\Delta|\gg G_T/\nu V_{\rm isl}$, with $V_{\rm isl}$ being the island's volume. Also, the size of the island, d, is supposed to be smaller than the superconductive coherence length so that for $T\ll T_c$ the only relevant degree of freedom in the island is the phase φ of the order parameter. In the Keldysh formalism, one has to introduce its classical, φ_1, and quantum, φ_2, components, and arranging them into a matrix $\check{\varphi}=\varphi_1\sigma_0+\varphi_2\sigma_x$ one can write Q_S in the subgap limit ($\epsilon<\Delta$) as

$$Q_S=-i\tau_+e^{i\check{\varphi}}+i\tau_-e^{-i\check{\varphi}}. \tag{2.8}$$

We will also consider below the example of a normal (nonsuperconductive) island connected to the film by a tunnel barrier and biased at some voltage with respect to it. In that case the island's Q matrix can also be formally expressed in terms of the superconductive phase:

$$Q_N=e^{i\tau_z\check{\varphi}/2}\Lambda e^{-i\tau_z\check{\varphi}/2}, \tag{2.9}$$

with $\varphi/2$ having the meaning of the single-particle phase which is conjugated to the number of electrons on the island (while φ is conjugated to the number of Cooper pairs). In both cases the applied voltage $V(t)$ can be accounted for by the Josephson relation $d\varphi_1/dt=2eV$ for the classical component of the phase.

FIG. 2. The second order in the γ correction to the action. The horizontal line schematically designates the N-S boundary Γ, with the two semicircles below it denoting Q_S in the island and the two-line object above it representing the Cooperon in the normal metal.

III. FUNCTIONAL RG: NONINTERACTING CASE

A. General idea

In this section we will apply the renormalization group treatment to the system consisting of a small island coupled to a diffusive metal film by a tunnel barrier of arbitrary transparency. The effects of the Cooper interaction in the film will be considered later on in Sec. V, while now we will study noninteracting electrons. In this section we will restrict ourselves to the *zero-energy limit* when both temperature T, voltage eV, and frequency ω are smaller that the Thouless energy $E_{\rm Th}=D/L^2$, and the perpendicular magnetic length $l_H=\sqrt{\Phi_0/H}$ (Φ_0 is the flux quantum and H is the applied magnetic field) is shorter than the system size L. The effect of larger T, V, or H is to destroy Cooperon coherence at scales larger than $\min\{\sqrt{D/T},\sqrt{D/eV},l_H\}$, and will be studied in Sec. VI. The effect of high-frequency ($\omega\gg E_{\rm Th}$) voltage is twofold: it suppresses Cooperon coherence and also perturbs the local electroneutrality of the electron system. We will not study this effect in the present paper.

The method developed in the present section can be applied to both the normal and superconductive islands. However, since the rest of the paper will be devoted mainly to the study of charge transport in the N-S system, all formulas will be written for the case of a superconducting island, $Q_{\rm isl}=Q_S$. In order to translate them for the case of a normal island, one has to substitute Q_S by Q_N and the word ''Cooperon'' by the word ''diffuson.''

Renormalization of the total action $S_{\rm bulk}+S_{\rm tun}$ describing an N-S contact is a complicated task. The main problem one encounters here is that this action does not reproduce itself under renormalization. In the lowest order over the tunneling transparency γ studied in Ref. 1, the boundary term (2.7) generates the next-order term $\gamma_2{\rm Tr}(Q_SQ)^2$ in the action, with γ_2 obeying the RG equation $d\gamma_2/d\zeta\propto\gamma^2$. The physical meaning of this relation is simple. It describes the process when a Cooper pair tunnels from the island, coherently propagates in the normal metal as a Cooperon, and then returns back to the island. The resulting expression is bilinear in Q_S (taken at the times of the first and second tunneling) and involves a logarithmically (in 2D) large factor due to the probability of returning to the original point. The corresponding diagram is shown in Fig. 2.

In order to clear up the structure of the leading logarithmic corrections at arbitrary interface transparencies, let us consider the diagrams of the fourth order over γ shown in Fig. 3. All of them ought to have *treelike* structure since any loop yields an additional small factor $\zeta/g\ll 1$. For two of them, labeled by (a) and (b), successive Andreev tunnelings are connected by free Cooperons and diffusons, whereas the

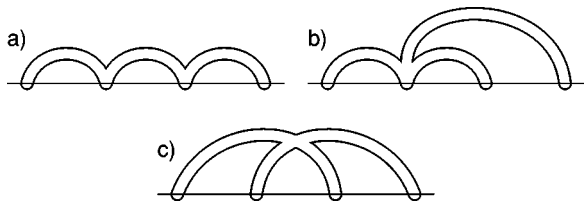

FIG. 3. Three leading logarithmic corrections to the action at the fourth order in γ.

process shown in Fig. 3(c) involves four-Cooperon interaction vertex (Hikami box) in the bulk. Due to spatial integration, each of these diagrams evaluates to the third power ζ^3 of the logarithm, and they exhaust the number of the most divergent diagrams of the fourth order.

Figure 3 suggests an idea that the treelike structure of corrections to the action may be suitable for the RG approach. Indeed, for each tree one can find the branch with the smallest momentum, say, q. If we cut the whole tree over this branch, it will break up into two pieces which could be calculated at the previous steps of the RG procedure since they contain only momenta greater that q. The diagrams (a) and (b) conform well to this scheme; however, it is not clear how to treat the bulk nonlinearity in the diagram (c). To overcome this problem we will employ our freedom to choose an arbitrary parametrization of the field Q in terms of the matrix W that can change the relative contribution of different diagrams. For the problem in question, the choice of the exponential parametrization, $Q=\Lambda\exp(W)$, nullifies all diagrams with Hikami boxes within the RG precision. To see this, we note that the leading logarithmic contribution arises from integration over the fast momentum, so that the energy dependence of the diffusion propagators (2.5) can be neglected. To this accuracy, the matrices W and ∇W commute and the term $\mathrm{Tr}(\nabla Q)^2=-\mathrm{Tr}(\nabla W)^2$ becomes Gaussian in W; therefore there are no nonlinear vertices in the bulk in the zero-energy limit. Note also that the same exponential parametrization is used usually for the solution of the Usadel equations[25,17] for the Green functions of disordered superconductors.

Thus, in the exponential parametrization, diagrams of the type shown in Fig. 3(c) are absent and one can carry out the RG procedure based on the treelike structure of the leading diagrams. Following this approach we present the total action as a sum of the bulk part S_{bulk} and the part S_Γ which arises from the single tunneling action (2.7) under renormalization:

$$S_\Gamma=\sum_{n=1}^{\infty}S_n=-i\pi^2 g\sum_{n=1}^{\infty}\gamma_n\mathrm{Tr}_\Gamma(Q_SQ)^n. \tag{3.1}$$

The renormalized boundary action (3.1) describes processes of multiple Andreev tunneling coupled by coherent propagation of two-particle diffusion modes in the normal metal. It is determined by the infinite set of coefficients (''charges'') γ_n and is a functional of the phase $\vec{\varphi}$ of the island's order parameter. Once γ_n's are known, one can easily calculate the Andreev conductance and other quantities related to charge transfer through the system (see Sec. IV B). Our main purpose below will be to establish the law of transformation of the coefficients γ_n and to derive the corresponding multicharge renormalization group equation.

B. Derivation of the multicharge RG equation

According to the general approach discussed above, at each step of the RG procedure one has to calculate a correction $\Delta S_{k,n}$ to the action which results from connecting two pieces S_k and S_n of the boundary action (3.1) by a fast diffusion mode. This gives a logarithmic contribution at scales larger than the island size d and, consequently, at energies Ω smaller than $\omega_d\equiv D/d^2$. Therefore in this case it is convenient to define the logarithmic variable as

$$\zeta=\ln\frac{\omega_d}{\Omega}=2\ln\frac{R}{d}, \tag{3.2}$$

where the current spatial scale R is related to Ω through $\Omega=D/R^2$. For the purposes of the RG, the form of the island is of no importance, and all expressions depend only on the total normal-state interface conductance G_T. Hence, one can formally consider a pointlike island, with the transparency γ in Eq. (2.7) becoming $\gamma=G_T$ and $\mathrm{Tr}_\Gamma X\equiv\mathrm{Tr}X(\mathbf{r}=0)$.

Our aim is to derive an effective low-energy action of the phase $\vec{\varphi}$ on the island; therefore we consider Q_S as a slow variable and decompose only metallic Q into the fast and slow parts. Such a decomposition consistent with the exponential parametrization adopted is given by $Q=\tilde{U}^{-1}\Lambda\exp(W')\tilde{U}$, where $\tilde{U}$ is a slow rotation matrix and W' is a fast variable.[1,15] The relevant interaction vertex reads

$$S_{\mathrm{int},n}=-i\pi^2 g n\gamma_n\mathrm{Tr}_\Gamma(Q_S\tilde{Q})^{n-1}Q_S\tilde{U}^{-1}\Lambda W'\tilde{U}, \tag{3.3}$$

where the additional factor of n accounts the fact that the fast diffusion mode can be coupled to any matrix Q in S_n, and $\tilde{Q}\equiv\tilde{U}^{-1}\Lambda\tilde{U}$. The form of the vertex (3.3) corresponds to the treelike structure of the diagrammatic expansion discussed in Sec. III A. The lack of higher-order terms in W in $S_{\mathrm{int},n}$ amounts to neglecting closed loops by virtue of the small parameter ζ/g.

For $k\neq n$, the correction to the action is given by $\Delta S_{k,n}=i\langle S_{\mathrm{int},k}S_{\mathrm{int},n}\rangle$. This average (in the zero-energy limit) is given by Eq. (A3), with

$$A=\tilde{U}(Q_S\tilde{Q})^{k-1}Q_S\tilde{U}^{-1}\Lambda, \tag{3.4a}$$

$$B=\tilde{U}(Q_S\tilde{Q})^{n-1}Q_S\tilde{U}^{-1}\Lambda. \tag{3.4b}$$

Calculating the logarithmic integral over the fast momentum, omitting the tilde sign over slow variables, employing invariance of the trace under cyclic permutations, and using the relations $Q^2=Q_S^2=1$, we get finally for $k\neq n$

$$\Delta S_{k,n}=\frac{i\pi^2 g}{2}kn\gamma_k\gamma_n\Delta\zeta\mathrm{Tr}_\Gamma[(Q_SQ)^{k+n}-(Q_SQ)^{|k-n|}]. \tag{3.5}$$

Thus we see that averaging of the terms S_k and S_n from the action (3.1) modifies the terms S_{k+n} and $S_{|k-n|}$ with $\Delta\gamma_{k+n}=-(1/2)kn\gamma_k\gamma_n\Delta\zeta$ and $\Delta\gamma_{|k-n|}=(1/2)kn\gamma_k\gamma_n\Delta\zeta$.

Analogous calculation of $\Delta S_{k,k}=(i/2)\langle S^2_{\mathrm{int},k}\rangle$ yields

$$\Delta S_{k,k}=\frac{i\pi^2 g}{4}k^2\gamma_k^2\Delta\zeta\mathrm{Tr}_\Gamma(Q_SQ)^{2k}, \tag{3.6}$$

which results in renormalization of the coefficient $\Delta\gamma_{2k}=-(1/4)k^2\gamma_k^2\Delta\zeta$.

Taking into account all possible pairings $\Delta S_{k,n}$ between the terms of the action (3.1), we derive the main equation that describes evolution of the charges γ_n under renormalization:

$$\frac{d\gamma_n}{d\zeta}=-\frac{1}{4}\sum_{k=1}^{n-1}k(n-k)\gamma_k\gamma_{n-k}+\frac{1}{2}\sum_{k=1}^{\infty}k(n+k)\gamma_k\gamma_{n+k}. \tag{3.7}$$

Initial conditions for these multicharge RG equations at $\zeta=0$ follow from the bare tunneling action (2.7):

$$\gamma_1(0)=a\equiv\frac{G_T}{4\pi g},\quad \gamma_{n>1}(0)=0. \tag{3.8}$$

Note that $Q_S^2=1$ is the only property of the island's Q_S which was used to derive the RG equations (3.7). Therefore these equations universally describe both normal-metal and superconductive islands on the same footing.

Equations (3.7) look quite complicated. Their hidden algebraic structure becomes transparent after Fourier transformation. To this end we introduce a 2π-periodic function $u(x)$ of an auxiliary continuous variable x according to the definition

$$u(x)=\sum_{n=1}^{\infty}n\gamma_n\sin nx. \tag{3.9}$$

Transforming Eq. (3.7) into an x representation we obtain the following RG equation for the function $u(x)$:

$$u_\zeta+uu_x=0. \tag{3.10}$$

The differential equation (3.10) is nothing but the well-known Euler equation describing 1D motion of a compressible gas, with ζ playing the role of time. The initial condition for Eq. (3.10) at $\zeta=0$ is given by $u_0(x)=a\sin x$.

The Euler equation (3.10) can be easily solved with the help of characteristics. The latter are described by the following system of differential equations:

$$\frac{dx}{d\zeta}=u,\quad \frac{du}{d\zeta}=0. \tag{3.11}$$

They are trivially integrated: $u=u_0(x_0)$ and $x=x_0+u_0(x_0)\zeta$. In order to get $u(x)=u_0(x_0(x))$ one has just to find the inverse function $x_0(x)$. For $u_0(x)=a\sin x$, the function $u(x)$ is implicitly defined by the relation

$$u(x)=a\sin[x-u(x)\zeta]. \tag{3.12}$$

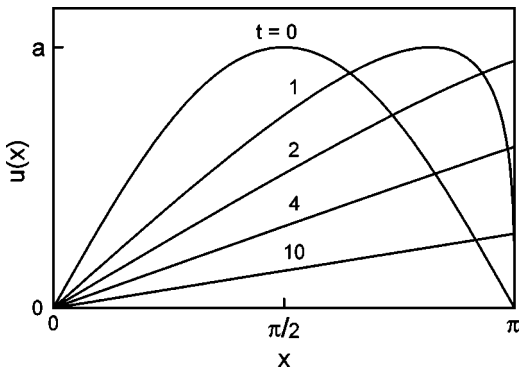

FIG. 4. Solutions for the Euler equation (3.10) at different values of $t=a\zeta$.

The solution of the Euler equation is conveniently expressed through the variable $t=a\zeta=G_T/G_D$ which is equal to the ratio of the tunneling conductance of the barrier G_T to the conductance of the metal film $G_D=4\pi g/\zeta$ at the current scale. The solution for different values of t is shown in Fig. 4. The derivative $u_x(\pi)$ diverges at $t=1$, exactly at the point where $G_D=G_T$. For $t>1$, the discontinuity (''shock wave'') develops at $x=\pm\pi$. For $t\gg1$, the solution acquires a sawlike type with $u(x)\simeq(a/t)x=(G_D/4\pi g)x$.

C. Proximity action

In the previous section we have established the transformation law for the coefficients γ_n of the multicharge action (3.1) under the action of the renormalization group. After eliminating diffusion modes up to some value of the logarithmic variable ζ, the action becomes a functional of the island's Q_S and $Q(R)$ in the film taken at the spatial scale $R\sim de^{\zeta/2}$ from the island. For a finite system bounded by a perfect metallic lead located at a distance L ($L\gg d$) from the island (see Fig. 1), renormalization of the action started at the energy scale ω_d should stop at the scale of the Thouless energy $E_{\mathrm{Th}}=D/L^2$ when all diffusive electronic degrees of freedom in the dirty metal are integrated out. The resulting action

$$S_{\mathrm{prox}}[Q_S,Q_N]=-i\pi^2 g\sum_{n=1}^{\infty}\gamma_n\mathrm{Tr}(Q_SQ_N)^n \tag{3.13}$$

thus becomes the functional of the island's Q_S, Eq. (2.8), and the matrix Q_N, Eq. (2.9), in the lead. Such an action resulting from elimination of the modes in the diffusive conductor will be referred to as the proximity action.

According to Eqs. (2.8) and (2.9), the only degree of freedom in the matrices Q_S and Q_N is the one associated with the phase rotation. In other words, externally controlled voltage is the only dynamical variable both in the island and in the lead. Below we will assume that the metal lead is at zero bias, so that Q_N reduces to Λ and the proximity action (3.13) acquires the form

$$S_{\mathrm{prox}}[Q_S]=-i\pi^2 g\sum_{n=1}^{\infty}\gamma_n\mathrm{Tr}(Q_S\Lambda)^n. \tag{3.14}$$

In this formula, γ_n are taken at ''time'' $t=a\zeta_{\rm Th}$, with $\zeta_{\rm Th} \equiv \ln(\omega_d/E_{\rm Th})=2\ln(L/d)$. It can be calculated through the integration of the FRG equation (3.10) for the function $u(x,\zeta)$ up to the scale $\zeta_{\rm Th}$.

In order to express the action in terms of the phase $\vec{\varphi}$, one has to substitute Q_S from Eq. (2.8). Taking the trace over Nambu space, we obtain that only terms with even n contribute to the proximity action:

$$S_{\rm prox}[Q_S]=-2i\pi^2 g\sum_{n=1}^{\infty}(-1)^n\gamma_{2n}{\rm Tr}_K(e^{i\vec{\varphi}}\Lambda_0 e^{-i\vec{\varphi}}\Lambda_0)^n, \tag{3.15}$$

where the subscript K indicates that the matrix trace is taken only over Keldysh space. As explained in Sec. III B, the action (3.14), after substitution $Q_S\to Q_N$, also applies to the case of the normal island. Using Eq. (2.9) for Q_N and taking the trace over Nambu space, we arrive at the following expression for the action:

$$S[Q_N]=-2i\pi^2 g\sum_{n=1}^{\infty}\gamma_n{\rm Tr}_K(e^{i\vec{\varphi}/2}\Lambda_0 e^{-i\vec{\varphi}/2}\Lambda_0)^n. \tag{3.16}$$

Remarkably, for the noninteracting case, our function $u(x,\zeta_{\rm Th})$ can be directly related to the generating function of transmission coefficients $F(\phi)$ introduced by Nazarov[4] (cf. also Ref. 22). Comparing our Eq. (3.12) with Nazarov's Eq. (19) one can verify that

$$4\pi^2 g u(x)=\int_0^1\frac{T\sin x}{1-T\sin^2(x/2)}\mathcal{P}(T)dT, \tag{3.17}$$

where $\mathcal{P}(T)$ is the distribution function of transmission coefficients normalized to the number of channels. Note also that the appearance of discontinuity in $u(x)$ for $t>1$ goes in parallel with the opening of conducting channels with transparencies $T\to 1$.[4] The sawlike solution for the function $u(x)$ at $t\gg 1$ results[4] in Dorokhov's[26] bimodal distribution function $\mathcal{P}(T)=\pi G_D/T\sqrt{1-T}$ for the transmission coefficients of a diffusive system.

It might be surprising to realize the equivalence of the two approaches since Nazarov's result is valid for any geometry while our FRG equation apparently holds only in 2D. Such a coincidence is related to the fact that both Nazarov's derivation and our derivation of the functional RG equation (3.10) implied the *zero-energy limit*, $T,eV,\omega<E_{\rm Th}$. Under this condition it is possible to derive the universal distribution of the eigenvalues of the transmission matrix as well as to neglect Cooperon decoherence in deriving Eq. (3.10). Note further that summation of the treelike diagrams for the action can be performed without the use of the RG at all: one has to integrate diffusion propagators over momentum independently for each branch of the tree. But in the zero-energy limit, such integration is expressed in terms of the Green function of the Laplace operator, thus reducing to the total resistance of the system. Therefore, in this case Eq. (3.10) rewritten in terms of $t=G_T/G_D$ remains valid for any geometry of the disordered normal region.

The power of the Keldysh multicharge proximity action will be crucial if one has to go beyond the zero-energy limit and, especially, for problems with the interaction. The corresponding FRG equations replacing the zero-energy-limit Euler equation (3.10) will be derived in Secs. VI and V.

IV. PHYSICAL QUANTITIES

Now we will discuss how the action (3.14) together with the FRG equation (3.10) valid in the zero-energy limit can be used to calculate physically observable quantities. In this section we will derive the general equations for the conductance and noise power in terms of the coefficients γ_n of the proximity action, and will apply them to the noninteracting case in order to demonstrate the functionality of the approach in use. Thereby we will recover the known results of Refs. 3–6 and 18. The equivalence comes from the fact that $\{\gamma_n\}$ carry the same information as the distribution function $\mathcal{P}(T)$ of the transmission coefficients of the system, so that one can calculate the conducting properties of the system with the help of the general formulas of Ref. 6.

Once the proximity action $S_{\rm prox}[Q_S]$ is known, the system conductance as well as the current statistics can be calculated following the method of Ref. 1. We will suppose that the island is connected to the voltage source by an ideal conductor so that phase fluctuations are suppressed (the effect of phase fluctuations will be studied elsewhere[27]). In this case the general expression $Z=\int D\varphi_1 D\varphi_2\exp\{iS_{\rm prox}[\varphi_1,\varphi_2]\}$ for the Keldysh partition function reduces to $Z=\exp\{iS_{\rm prox}[\varphi_{s1},\varphi_{s2}]\}$ where $\vec{\varphi}_s$ is the island's phase controlled by the source. The dynamics of its classical component is governed by the applied voltage through the Josephson relation $d\varphi_{s1}/dt=2eV(t)$, while the current operator is given by the derivative with respect to the quantum component of the phase:

$$\hat{I}(t)=ie\frac{\delta}{\delta\varphi_{s2}(t)}. \tag{4.1}$$

In order to obtain the expectation value of currents taken at different moments of time one should apply the operators (4.1) to $\ln Z$:

$$\langle I(t_1)\cdots I(t_k)\rangle=\hat{I}(t_1)\cdots\hat{I}(t_k)\ln Z[\varphi_{s1},\varphi_{s2}]\big|_{\varphi_{s2}=0}. \tag{4.2}$$

Below we will employ these relations to calculate the conductance and noise for the case of the normal and superconductive islands.

A. Normal junction: Conductance and noise

To illustrate the formalism, we start by considering the conductance of the system for the case of the normal island. We will trace how addition of resistances R_T and R_D is realized within the multicharge action approach and calculate the current noise power.

In order to calculate the current response $\langle I\rangle$ to the bias voltage V one has to employ Eqs. (3.16), (4.1), and (4.2).

Evaluating the functional derivative with the help of Eq. (B5) we obtain for the dimensionless conductance $G=(\hbar/e^2)\langle I\rangle/V$

$$G=4\pi g\sum_{n=1}^{\infty} n^2\gamma_n=4\pi g u_x(0). \tag{4.3}$$

According to the Euler equation (3.10), G obeys $\partial G^{-1}/\partial\zeta=1/4\pi g$, which amounts to the anticipated addition of resistances:

$$G=\frac{G_T}{1+t}=\frac{G_T G_D}{G_T+G_D}, \tag{4.4}$$

where

$$G_D=\frac{2\pi g}{\ln(L/d)} \tag{4.5}$$

is the metal film conductance between the island and the lead.

Equation (4.4), though derived in the low-frequency limit $\omega\ll D/L^2$, can be shown to remain valid for much larger frequencies, up to $\omega_{\max}=2\pi\sigma/L$ (for the bare Coulomb interaction) or $\omega_{\max}=4\pi\sigma/b$ (if the Coulomb interaction is screened by the presence of a gate situated at the distance b from the film; see Sec. II). This frequency determines the time scale $\omega_{\max}^{-1}$ at which the electroneutrality of the system sets in.

After this example let us turn to a more involved calculation of the current-current correlator at a fixed constant bias V. Now one has to apply two current operators (4.1) to the action (3.16). The corresponding functional derivative is calculated in Appendix B. Substituting it from Eq. (B10) and employing Eq. (4.3) one obtains

$$\langle I_\omega I_{-\omega}\rangle=\frac{e^2G}{3\hbar}\left\{(3-P_N(t))\Psi(\omega)+\frac{1}{2}P_N(t)[\Psi(\omega-eV)+\Psi(\omega+eV)]\right\}, \tag{4.6}$$

with the function $\Psi(\omega)$ defined as

$$\Psi(\omega)\equiv\int_0^\infty[1-F(E_+)F(E_-)]dE=\omega\coth\frac{\omega}{2T}, \tag{4.7}$$

where $E_\pm=E\pm\omega/2$. The function $P_N(t)$ is given by

$$P_N(t)=1+\frac{2\sum_{n=1}^{\infty} n^4\gamma_n}{\sum_{n=1}^{\infty} n^2\gamma_n}=1-\frac{2u_{xxx}(0)}{u_x(0)}. \tag{4.8}$$

The third derivative $u_{xxx}(0)$ can be easily calculated with the help of characteristics. The one reaching the point $x=0$ is obviously $x(\zeta)=0$ with $x_0=0$. Writing $u(x)=u_0(x_0)$ and using the relation $\partial_x=[1+t\cos x_0]^{-1}\partial_{x_0}$ at $x_0=0$ we obtain

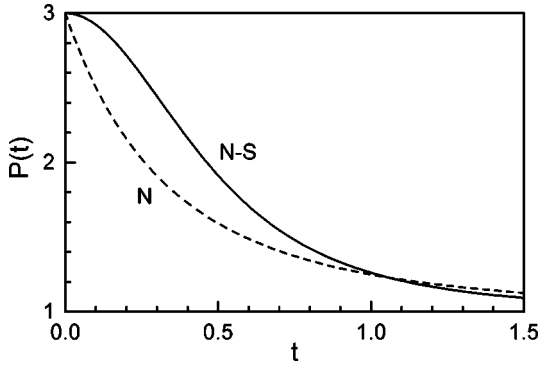

FIG. 5. Noise functions $P_N(t)$ (dashed line) and $P_S(t)$ (solid line) for normal and N-S junctions, correspondingly, vs the ratio $t=G_T/G_D$.

$$u_{xxx}(0)=-\frac{a}{(1+t)^4}=-\frac{1}{4\pi g}\frac{G^4}{G_T^3}, \tag{4.9}$$

and, therefore,

$$P_N(t)=1+2\frac{G^3}{G_T^3}. \tag{4.10}$$

Equations (4.6) and (4.10) provide a general description of the noise power for an arbitrary relation between the frequency (which should be smaller than $E_{\rm Th}$), voltage, and temperature, and arbitrary R_T/R_D. Though it was derived in the zero-energy limit, the condition $(T,eV)<E_{\rm Th}$ can be relaxed since, for a normal island, charge propagation in the diffusive conductor is described in terms of diffusons which are insensitive to decoherence.

In the limit $V\to 0$, Eq. (4.6) reduces to the Nyquist-Johnson equilibrium thermal noise

$$\langle I_\omega I_{-\omega}\rangle_{\rm Nyq}=\frac{e^2G}{\hbar}\omega\coth\frac{\omega}{2T}. \tag{4.11}$$

In the limit $eV\gg(\omega,T)$, one obtains for the shot noise power

$$\langle II\rangle_{\rm shot}=\frac{e^2G}{3\hbar}P_N(t)eV, \tag{4.12}$$

which coincides with Nazarov's result[4] obtained via the distribution function of transmission coefficients. According to Eq. (4.12), the Fano factor[20] of the system measuring the reduction of shot noise compared to its Poissonian value is given by $F_N=P_N/3$. The function $P_N(t)$ is plotted in Fig. 5 by the dashed line. For $t\gg 1$, when the system resistance is dominated by the diffusive conductor, the shot noise power is 3 times smaller than its Poisson value. This result was first obtained in Ref. 28 with the help of Dorokhov's bimodal distribution,[26] and in Ref. 29, in the framework of the classical Boltzmann equation with Langevin sources.

The proximity action (3.14) together with the FRG equation (3.10) allows, in principle, for the calculation of higher momenta of current fluctuations and even the full statistics of transmitted charge (cf. Refs. 30 and 31). We leave this problem for future investigation.

B. Andreev conductance

In this section we will turn to the case of a superconductive island. We will assume that the island is not very small so that its order parameter satisfies $\Delta > \omega_d$. This means that at the scales $\Omega < \omega_d$ relevant for the RG, quasiparticle reflection from the island is of Andreev type and one can use the subgap expression (2.8) for the island's Q_S.

We write the current as a sum of the partial contributions $\langle I(t)\rangle_n$ from different terms of the action (3.15):

$$\langle I(t)\rangle_n = (-1)^n 2ie\pi^2 g\gamma_{2n} \left.\frac{\delta \mathrm{Tr}_K(e^{i\vec{\varphi}}\Lambda_0 e^{-i\vec{\varphi}}\Lambda_0)^n}{\delta\varphi_2(t)}\right|_{\varphi_2=0}. \tag{4.13}$$

Calculating the derivative with the help of Eq. (B4) we find for the dimensionless Andreev conductance

$$G_A = 16\pi g \sum_{n=1}^{\infty} (-1)^n n^2 \gamma_{2n} = 4\pi g u_x\left(\frac{\pi}{2}\right). \tag{4.14}$$

Note that Eqs. (4.3) and (4.14) for the case of the normal and superconducting islands look very similar. The only difference is at the point where the derivative should be taken.

Now we will use the general expression (4.14) to calculate G_A in the noninteracting case. The simplest way to get $u_x(\pi/2)$ is to use the characteristics of the Euler equation (3.10). We have to find the one which leads to $x=\pi/2$ at ''time'' t. Writing its initial point as $x_0 = \pi/2 - \Theta(t)$ we obtain the following equation for the function $\Theta(t)$:

$$\Theta(t) = t\cos\Theta(t). \tag{4.15}$$

For small t, $\Theta(t \ll 1) = t + O(t^3)$ while in the limit of large t, $\Theta(t \gg 1) = \pi/2 - \pi/2t + O(t^{-2})$. Now, applying $\partial_x = [1 + t\cos x_0]^{-1}\partial_{x_0}$ to $u(x) = u_0(x_0)$ we obtain

$$u_x\left(\frac{\pi}{2}\right) = \frac{a\sin\Theta(t)}{1+t\sin\Theta(t)} \tag{4.16}$$

and, finally,

$$G_A = G_T \frac{\sin\Theta(t)}{1+t\sin\Theta(t)} = G_D \frac{t\sin\Theta(t)}{1+t\sin\Theta(t)}, \tag{4.17}$$

where G_D is defined in Eq. (4.5).

In terms of the resistance, the zero-energy result (4.17) can be written as

$$R_A = R_D + R_{T,\mathrm{eff}}, \tag{4.18}$$

where $R_{T,\mathrm{eff}}(t) = R_T/\sin\Theta(t)$ has the meaning of an effective interface resistance connected in series with the metal-film resistance $R_D = (\hbar/e^2)G_D^{-1}$. The former decreases with the increase of R_D due to disorder-induced enhancement of Andreev reflection determined by the probability of returning to the origin.

Equation (4.17) for the Andreev conductance had been previously derived by Volkov *et al.*,[3] and rederived later by Nazarov both with the help of the Usadel equation[5] and the generating function of transmission eigenvalues.[4] This latter approach, though formulated in a very different language, appears to be directly connected to our multicharge action approach. Using the relation between $u(x)$ and distribution of transmission coefficients established in Eq. (3.17) for the noninteracting limit, one can reduce Eq. (4.14) to the sum over conducting channels: $G_A = \pi^{-1}\Sigma_n T_{An}$, where $T_{An} = 2T_n^2/(2-T_n)^2$. This equation is nothing but the generalization of the Landauer formula to the case of N-S systems derived by Beenakker.[32]

C. Noise of NS current

Decomposing the current-current correlator into the sum of the partial contributions, $\langle I_\omega I_{-\omega}\rangle_n$, similarly to Eqs. (4.13), using Eq. (B9), and employing Eq. (4.14) we obtain

$$\langle I_\omega I_{-\omega}\rangle = \frac{e^2 G_A}{3\hbar}\left\{[3 - P_S(t)]\Psi(\omega) + \frac{1}{2}P_S(t)[\Psi(\omega - 2eV) + \Psi(\omega + 2eV)]\right\}, \tag{4.19}$$

where $\Psi(\omega)$ is defined in Eq. (4.7). The superconductive noise function $P_S(t)$ is given by

$$P_S(t) = 1 + \frac{2\sum_{n=1}^{\infty}(-1)^n n^4 \gamma_{2n}}{\sum_{n=1}^{\infty}(-1)^n n^2 \gamma_{2n}} = 1 - \frac{u_{xxx}(\pi/2)}{2u_x(\pi/2)}. \tag{4.20}$$

Equation (4.19) has the same form as its analog for the N island with the replacement $P_N(t) \to P_S(t)$ and $eV \to 2eV$. The origin of this analogy was clarified by Muzykantskii and Khmelnitskii[33] who showed that the whole N-S counting statistics in the noninteracting case can be obtained from the counting statistics of normal electrons by replacing $T_n \to T_{An}$ and doubling the charge quantum $e \to 2e$.

For the noninteracting system, the value of $u_x(\pi/2)$ was calculated in Eq. (4.16), and calculating $u_{xxx}(\pi/2)$ in the same way we obtain

$$u_{xxx}\left(\frac{\pi}{2}\right) = -\frac{a\sin\Theta(t)}{[1+t\sin\Theta(t)]^4} - \frac{3at\cos^2\Theta(t)}{[1+t\sin\Theta(t)]^5}. \tag{4.21}$$

Thus, we get

$$P_S(t) = 1 + \frac{1 + \Theta\tan\Theta + 3\Theta\cot\Theta}{2[1+\Theta\tan\Theta]^4}, \tag{4.22}$$

where $\Theta \equiv \Theta(t)$ is defined in Eq. (4.15).

In the limit of vanishing bias, Eq. (4.19) with $P_S(t)$ from Eq. (4.22) reproduces the Nyquist-Johnson thermal noise given by Eq. (4.11), with G being substituted by G_A, Eq. (4.17). In the opposite limit of large bias, $eV \gg (\omega, T)$, it gives the power of the shot noise between the normal and superconducting terminals[18]:

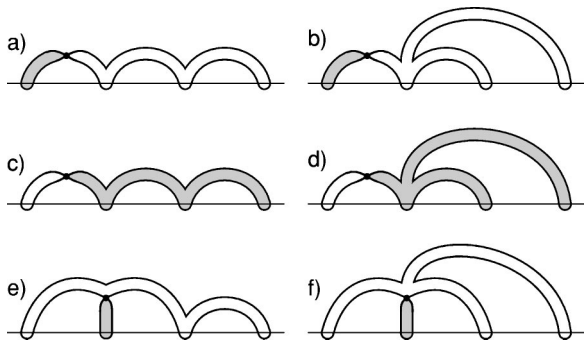

FIG. 6. Leading diagrams in the fourth order in γ and the first order in λ. Shadowed is the piece of the diagram where the logarithmic contribution of the Cooperon adjacent to the λ vertex results from the energy integration.

$$\langle II\rangle_{\rm shot}=\frac{2e^2G_A}{3\hbar}P_S(t)eV, \tag{4.23}$$

with the Fano factor $F_S=2P_S/3$. The function $P_S(t)$ is plotted in Fig. 5 together with its analog for the normal junction $P_N(t)$. On increasing t, both $P_N(t)/3$ and $P_S(t)/3$ evolve from the value of 1 describing the Poisson noise at a tunnel contact to 1/3 corresponding to the diffusive conductor. An excess factor of 2 in Eq. (4.23) accounts the fact that in an N-S system charge is transferred by Cooper pairs. Our results agree with the results of Refs. 18 and 33.

The results obtained in Secs. IV B and IV C refer to the zero-energy limit. In Sec. VI we will extend our theory to the case of large temperature or voltage, $\max(T,eV)>E_{\rm Th}$.

V. EFFECT OF AN INTERACTION IN THE COOPER CHANNEL

A. General idea

Here we calculate the effect of repulsion in the Cooper channel on the renormalization of the effective boundary action (3.1). In the lowest order over the interface transparency, the RG equation for γ_1 was derived in Ref. 1. We will extend this result to account for the whole set of charges $\{\gamma_n\}$.

As in Sec. III, we first turn to the analysis of the lowest-order perturbative corrections to the action. The Cooper-channel interaction is described by the following vertex in the bulk action:

$$S_\lambda=\frac{\pi^2\nu\lambda}{4}\int d\mathbf{r}dt\,{\rm tr}\sigma_x[Q^2-(\tau_zQ)^2], \tag{5.1}$$

obtained from the σ-model action (2.1) by eliminating the fluctuating $\vec{\Delta}$ field.[1] The treelike diagrams for the action of the noninteracting system should be modified now by all possible insertions of the vertexes S_λ. In the lowest order in the interface transparency γ (cf. Fig. 2), that was carried out in Ref. 1. The diagrams of the fourth order in γ and the first order in λ are shown in Fig. 6. They are obtained from the diagrams of Fig. 3 by insertions of the Cooper vertex denoted by a dot. The latter cuts a diagram into two parts with independent energy integration variables.

The leading logarithmic contribution of a diagram from Fig. 6 is due to the *momentum* integration in each diffusion mode except for one of the Cooperons adjacent to the vertex S_λ, whose contribution is logarithmic due to the *energy* integral $\int dE/E$. The corresponding part of the diagram containing such a Cooperon is shadowed in Fig. 6. Thus, each of the diagrams shown in Fig. 6 evaluates to the fourth power of the logarithm, $\propto\lambda\gamma^4\zeta^4$.

To achieve this situation, the energy E and momenta in the shadowed part of the diagram must obey some inequalities. First, the momentum of the Cooperon adjacent to the λ vertex, q, must satisfy the relation $Dq^2<E$. Second, momenta of all other shadowed Cooperons, q_i, must satisfy the relation $Dq_i^2>E$. Only under these conditions does the diagram evaluate to the maximal power of the logarithmic variable ζ.

Were all diffusion modes in the shadowed region of the diagram Cooperons, the energy E would be the slowest variable in this region. Then, on the level of the RG, the shadowed region would be taken into account by the pairing of the vertex S_λ with the multicharge action S_Γ [Eq. (3.1)] obtained at the previous steps of the RG procedure. Since E would be the slowest variable in the shadowed part, all metallic Q's entering the action S_Γ paired to S_λ should be set to Λ, indicating that no further pairings with slower variables are allowed to the shadowed region. As a result, as will be shown in Sec. V B, the shadowed region will give a correction to the term $S_1\propto\gamma_1{\rm Tr}_\Gamma Q_SQ$. However, the shadowed region might contain diffusons as well. Their momenta q_i are not restricted by the inequality $Dq_i^2>E$ and may be ''slower'' than the energy E. Were this the case, the multicharge action (3.1) would not reproduce itself upon pairing with S_λ since one would not be able to perform the integration over E as the result would depend on the next steps of the RG.

Fortunately, the diffuson contribution in the shadowed part of a diagram can be disregarded. This can be seen already from the diagrams of the fourth order shown in Fig. 6. Among them only diagram (c) contains a shadowed diffuson. However, direct calculation shows that its contribution to the action vanishes identically.[34] This statement can be generalized to arbitrary order. One can prove that any diagram containing a diffuson in the shadowed region is exactly zero. Physically, the shadowed part of a diagram accounts the correction to the Usadel spectral angle θ (cf. Appendix C) which is determined solely by Cooperon modes.

B. Functional RG equation

To calculate the correction to the action due to the pairing $S_{n,\lambda}=i\langle S_{{\rm int},n}S_{{\rm int},\lambda}\rangle$ one should extract one fast W' from S_λ,

$$S_{{\rm int},\lambda}=\frac{\pi^2\nu\lambda}{4}{\rm Tr}\{\sigma_x,\tilde{Q}\}\Lambda(W'-\tau_zW'\tau_z), \tag{5.2}$$

and another one from S_n according to Eq. (3.3). The only fast variable to be integrated out at this step of the RG procedure is the energy E running over the Cooperon propagator $\langle W'W'\rangle$. This fast energy runs also over all $\tilde{Q}$'s under the

trace in $S_{\mathrm{int},n}$. Substituting $\tilde{Q}=\Lambda(E)$ into Eq. (3.3) as explained above and performing the averaging over the fast Cooperon in $\langle S_{\mathrm{int},n}S_{\mathrm{int},\lambda}\rangle$ with the use of Eq. (A2), we obtain that only the terms with odd n give a nonzero contribution to the action (hereafter the tilde sign over slow variables is omitted):

$$S_{n,\lambda}=(-1)^{(n-1)/2}\frac{i\pi^3 gn\gamma_n\lambda}{4}\int_\Gamma d\mathbf{r}\int\frac{dtdE'dE}{(2\pi)^2E}$$
$$\times\mathrm{tr}\{[Q_S\Lambda_0(E)]^n+[\Lambda_0(E)Q_S]^n,\sigma_x\}Q. \quad (5.3)$$

Since E is a fast variable, all $Q_S(t)$ are taken at the same time t, and $Q=\int e^{i\omega t}Q_{E'-\omega/2,E'+\omega/2}(d\omega/2\pi)$. The sign in the above equation comes from commutation of τ_z contained in $\Lambda=\Lambda_0\tau_z$ with Q_S in order to transform $(Q_S\Lambda)^n$ to $(Q_S\Lambda_0)^n$.

Let us calculate

$$\mathcal{M}_n=\{(Q_S\Lambda_0)^n+(\Lambda_0Q_S)^n,\sigma_x\}, \quad (5.4)$$

which enters Eq. (5.3). It can be written as $\mathcal{M}_n=\{X^n+X^{-n},\sigma_x\}$, where $X=Q_S\Lambda_0$. According to Eq. (2.8), Q_S contains the classical and quantum parts: $Q_S=p+q\sigma_x$. Then it is easy to show that $\mathcal{M}_1=4Q_SF(E)$. Now we will show by induction that for all odd n, $\mathcal{M}_n=\mathcal{M}_1$. Consider the difference $\mathcal{M}_{n+2}-\mathcal{M}_n$. It contains $X^{n+2}-X^n-X^{-n}+X^{-n-2}=(X^{n+1}-X^{-n-1})(X-X^{-1})=\mathcal{F}(X)(X-X^{-1})^2$. Within RG accuracy, the distribution function $F(E)=\mathrm{sgn}E$ so that $F^2=1$. Under this condition, $(X-X^{-1})^2\equiv[Q_S,\Lambda_0]^2=0$, which proves the statement $\mathcal{M}_n=\mathcal{M}_1$.

Substituting

$$\{[Q_S\Lambda_0(E)]^n+[\Lambda_0(E)Q_S]^n,\sigma_x\}=4Q_S\mathrm{sgn}E \quad (5.5)$$

into Eq. (5.3), we get

$$S_{n,\lambda}=(-1)^{(n-1)/2}i\pi^3gn\gamma_n\lambda\Delta\zeta\mathrm{Tr}_\Gamma Q_SQ. \quad (5.6)$$

Therefore, only S_1 is subject to renormalization by the λ term:

$$\left(\frac{d\gamma_1}{d\zeta}\right)_{\text{due to }\lambda}=-\lambda\sum_{l=0}^{\infty}(-1)^l(2l+1)\gamma_{2l+1}. \quad (5.7)$$

As a result, an additional term will appear on the RHS of the Euler equation (3.10):

$$u_\zeta+uu_x=-\lambda(\zeta)u\left(\frac{\pi}{2}\right)\sin x. \quad (5.8)$$

Here $\lambda(\zeta)$ is described by the bulk RG equation (2.6) derived in the absence of the tunnel coupling between the island and the film. Note, however, that in the presence of tunneling, the real Cooper interaction vertex in the film, λ_{film}, will be additionally modified by Andreev reflections from the N-S boundary. Nevertheless, Eq. (5.8) should contain the bare bulk $\lambda(\zeta)$. The reason is that within our multicharge RG approach, all effects of the N-S interface are explicitly incorporated into the boundary action (3.1). Therefore, at each step of the RG procedure, one has to couple the renormalized boundary action, which already contains the logarithmic contribution of Cooperons integrated over fast $E>\Omega$, to the Cooper interaction vertex *without* Andreev reflection processes from the island, i.e., to the *bare* $\lambda(\zeta)$. This procedure ensures that no double counting of diagrams occurs in proceeding with the RG, and leads to Eq. (5.8).

The explicit dependence $\lambda(\zeta)$ can be easily found[15,1] from Eq. (2.6):

$$\lambda(\zeta)=\frac{\lambda_d+\lambda_g\tanh\lambda_g\zeta}{1+\frac{\lambda_d}{\lambda_g}\tanh\lambda_g\zeta}, \quad (5.9)$$

where $\lambda_g=1/2\pi\sqrt{g}$, λ_d is defined at the energy scale ω_d [cf. the definition (3.2) of the logarithmic variable ζ],

$$\lambda_d=\frac{\lambda_n+\lambda_g\tanh\left(\lambda_g\ln\frac{1}{\omega_d\tau}\right)}{1+\frac{\lambda_n}{\lambda_g}\tanh\left(\lambda_g\ln\frac{1}{\omega_d\tau}\right)}, \quad (5.10)$$

and λ_n is the interaction constant at the energy scale $\hbar/\tau$.

C. Andreev conductance

Here we consider the effect of repulsive interaction in the Cooper channel of a normal conductor on the Andreev conductance, in two limiting cases of weak and strong interactions. Of course, we always assume that the dimensionless coupling constant $\lambda\ll1$. We will see below that the limit of a strong interaction means $\lambda\gg G_T/4\pi g$, and thus can be realized at a relatively poor transparency of the interface. However, we will see also that even the weak-λ solution produces the interaction-induced correction to G_A which grows logarithmically with the spatial scale L and eventually crosses over to the strong-coupling limit where the nonperurbative treatment should be carried out.

Wherever possible we will perform an analytical calculation for an arbitrary relation between λ_d and λ_g. Otherwise we will assume that $\lambda(\zeta)$ had already reached Finkelstein's fixed point $\lambda_g=1/2\pi\sqrt{g}$, which is valid if either λ_n is of the order of λ_g or $\ln(1/\omega_d\tau)>\sqrt{g}$.

1. First-order correction

We start by treating the RHS of Eq. (5.8) perturbatively. The equations for the characteristics of Eq. (5.8) have the form

$$\frac{dx}{d\zeta}=u,\quad \frac{du}{d\zeta}=-\lambda(\zeta)u\left(\frac{\pi}{2},\zeta\right)\sin x. \quad (5.11)$$

The presence of $u(\pi/2,\zeta)$ in Eq. (5.11) which is determined by the trajectory reaching $x=\pi/2$ in ''time'' ζ introduces a nonlocal in ζ coupling between different trajectories. In the lowest order over $\lambda(\zeta)$, we search for a solution in the form $x(\zeta)=x_0+a\zeta\sin x_0+\delta x(\zeta)$ and $u(\zeta)=a\sin x_0+\delta u(\zeta)$, where δx and δu are proportional to λ and vanish at $\zeta=0$. Substituting this into Eqs. (5.11) and keeping only terms linear in λ, we obtain

$$\delta x(\zeta) = -a\int_0^\zeta (\zeta-\eta)\lambda(\eta)\cos[\Theta(a\eta)] \times \sin[x_0 + a\eta\sin x_0]d\eta, \tag{5.12}$$

$$\delta u(\zeta) = -a\int_0^\zeta \lambda(\eta)\cos[\Theta(a\eta)]\sin[x_0 + a\eta\sin x_0]d\eta. \tag{5.13}$$

Thereby, we know the characteristics of Eq. (5.8) in the first order over $\lambda(\zeta)$. As we have already seen in Sec. IV B, in order to calculate the Andreev conductance $G_A = 4\pi g u_x(\pi/2)$, one has to search for the characteristic which leads to $x=\pi/2$ in ''time'' ζ. Resolving equation $x(\zeta)=\pi/2$ we find that the initial point of such a trajectory, $x_0 = \pi/2 - \Theta(a\zeta) + \delta x_0$, gets shifted by

$$\delta x_0 = \frac{a}{1+a\zeta\sin\Theta(a\zeta)} \times \int_0^\zeta (\zeta-\eta)\lambda(\eta)\cos[\Theta(a\eta)]\cos\left[\Theta(a\zeta)\left(1-\frac{\eta}{\zeta}\right)\right]d\eta \tag{5.14}$$

compared to the noninteracting case. A nonzero λ influences the derivative $u_x(\pi/2) = (\partial u/\partial x_0)/(\partial x/\partial x_0)$ which determines the Andreev conductance in two ways. The first correction $\delta^{(1)}u_x(\pi/2)$ to the quasiclassical result (4.16) is related to the change of the initial point x_0 of the trajectory. The second correction $\delta^{(2)}u_x(\pi/2)$ is due to the modification of the functional dependences of $x(\zeta)$ and $u(\zeta)$ versus x_0 by the terms (5.12) and (5.13). A straightforward calculation yields

$$\delta^{(1)}u_x\left(\frac{\pi}{2}\right) = -\frac{a\cos\Theta(a\zeta)}{[1+a\zeta\sin\Theta(a\zeta)]^2}\delta x_0 \tag{5.15}$$

and

$$\delta^{(2)}u_x\left(\frac{\pi}{2}\right) = -\frac{a}{[1+a\zeta\sin\Theta(a\zeta)]^2}\int_0^\zeta \lambda(\eta) \times\cos[\Theta(a\eta)]\cos\left[\Theta(a\zeta)\left(1-\frac{\eta}{\zeta}\right)\right] \times[1+a\eta\sin\Theta(a\zeta)]^2 d\eta. \tag{5.16}$$

Finally, with the help of Eq. (4.14) we obtain for the Andreev conductance in the lowest order over the Cooper-channel interaction $\lambda(\zeta)$

$$\frac{G_A}{G_D} = \frac{t\sin\Theta(t)}{1+t\sin\Theta(t)} - \frac{\Theta(t)}{[1+t\sin\Theta(t)]^3}\zeta \times\int_0^1 \lambda(x\zeta)(1-x)\frac{\Theta(xt)}{x}\cos[\Theta(t)(1-x)]dx - \zeta\int_0^1 \lambda(x\zeta)\frac{[1+xt\sin\Theta(t)]^2}{[1+t\sin\Theta(t)]^2}\frac{\Theta(xt)}{x} \times\sin[\Theta(t)(1-x)]dx. \tag{5.17}$$

It is instructive to compare Eq. (5.17) with the result of the standard calculation of G_A by means of a direct solution of the Usadel equations. The first perturbative correction to G_A due to λ has been studied in Ref. 17 in 1D geometry, and we present a generalization of their approach to the 2D case of Fig. 1 in Appendix C. The resulting expression (C19) looks pretty similar to Eq. (5.17). The difference is that Eq. (5.17) contains, in general, the renormalized coupling constant $\lambda(\zeta)$ which depends on the energy scale through Eq. (5.9), while the result (C19) is expressed in terms of the bare coupling constant λ_d defined at the scale ω_d; cf. Eq. (5.10). Therefore, even on the level of the first correction the results of the functional RG treatment, Eq. (5.17), and of the Usadel approach, Eq. (C19), are somewhat different, with the former carrying more information. The main difficulties one encounters proceeding with the Usadel equation are outlined below.

The Usadel equation contains, in principle, the logarithmic dependence of $\lambda(\zeta)$ which follows from the first term of Eq. (2.6) in the absence of a Finkelstein correction: $\lambda(\zeta) = \lambda_d/(1+\lambda_d\zeta)$. It emerges as a result of the self-consistent determination of the proximity-induced Δ in the normal metal; cf. Eq. (C3). However, in order to take these effects into account within the approach presented in Appendix C, it would be necessary to solve the whole problem with higher-order accuracy in λ_d, which seems to be an extremely complicated task. The main complication is the appearance of the supercurrent flowing in the normal region that leads to the rotation of the phase $\varphi(\mathbf{r})$ of the anomalous Green function and also mixes both components f and f_1 of the distribution function. As a consequence, the problem becomes hardly tractable.

In the interacting case, the situation with the quasiclassical approach becomes much more involved, as one has to supply the Usadel equation with the equation for the electric potential. As a result, the whole system of kinetic equations becomes so complicated that its solution presents not a technical but rather a conceptual problem. Therefore, our approach seems to be the only tool to study the effect of the Cooper channel interaction on the conducting properties of 2D N-S systems.

Staying within first-order accuracy over λ_d, we identify $\lambda(\zeta)\equiv\lambda_d$ and find exact agreement between Eqs. (5.17) and (C19). Moreover, two contributions to the correction to G_A given by Eqs. (5.15) and (5.16) have their direct counterparts within the Usadel method: the first one is due to the modification of the spectral angle $\theta(r=d)$ [cf. Eq. (C10)], whereas the second one is, physically, due to the correction to the distribution function $f_1(r=L)$ by the presence of the induced Δ [cf. Eq. (C18)].

The somewhat cumbersome expression (5.17) can be simplified in the limiting cases of small and large t. For $t\ll 1$, the noninteracting Andreev conductance $G_A^{(0)}\approx G_T^2/G_D$, and one has for the interaction correction $\delta G_A \equiv G_A - G_A^{(0)}$

$$\frac{\delta G_A}{G_A} = -2\zeta\int_0^1 \lambda(x\zeta)(1-x)dx. \tag{5.18a}$$

In the opposite limit $t \gg 1$, the conductance is determined by the diffusive conductor, $G_A^{(0)} \approx G_D$, and

$$\frac{\delta G_A}{G_A} = -\frac{\pi}{2}\zeta \int_0^1 \lambda(x\zeta) x \cos\frac{\pi x}{2} dx. \tag{5.18b}$$

An important consequence of Eqs. (5.18) is that the relative value of the λ correction to the subgap conductance is proportional to $\lambda\zeta$ at any value of G_T/G_D, including the case of a completely transparent interface with $G_T^{-1}=0$. Thus, our result differs from the one obtained by Stoof and Nazarov[17] who considered the same kind of problem in the 1D geometry and found a weak regular correction $\sim \lambda$ only. The growth of the interaction-induced correction in 2D indicates that qualitative changes in the behavior of the function $u(x)$ do occur at large enough scales ζ and one has to sum the leading logarithmic terms, $(\lambda\zeta)^n$.

In the most general case of arbitrary $\lambda(\zeta)$, the FRG equation (5.8) should be solved numerically. However, in the limiting cases of *strong* and *weak* Cooper interactions, an analytical solution can be obtained. The former refers to the situation when the first correction, Eq. (5.18a), becomes of the order of 1 already in the limit of weak transparency of the barrier, $t \ll 1$. The latter applies when the first correction, Eq. (5.18b), becomes important only in the diffusive regime, $t \gg 1$. The boundary between the limits of strong and weak repulsion in the Cooper channel slightly depends on the relation between λ_d and λ_g. In the rest of this section we will consider the case when $\lambda_d \sim \lambda_g$. Then repulsion is strong (weak) provided that $\lambda_g \gg a$ ($\lambda_g \ll a$). We want to emphasize that the notion of strong and weak interactions refers not to the value of λ itself but to the ratio $\lambda/a = 4\pi g\lambda/G_T$. In both cases the interaction correction can be either small or large depending on the value of $\lambda\zeta = 4\pi g\lambda/G_D$.

The limiting cases of strong and weak repulsion will be considered in Secs. V C 2 and V C 3, and then (in Sec. V C 4) we will turn to the discussion of the general case of arbitrary λ.

Equations (5.18) describe the interaction correction to the total resistance of the system. It is instructive to study also the correction to the effective interface resistance defined in Eq. (4.18). In the limit of strong repulsion, this correction is determined by Eq. (5.18a). In the limit of weak repulsion, $R_{T,\mathrm{eff}} = R_T/\sin\Theta(t) \approx R_T$ is only a small part of R_A at $t \gg 1$. The λ term is also a small correction if $t \ll a/\lambda_g$. Expanding Eq. (5.17) in the region $1 \ll t \ll a/\lambda_g$ and assuming for simplicity that $\lambda(\zeta) = \lambda_g$, one obtains

$$\frac{R_{T,\mathrm{eff}}}{R_T} \approx 1 + \frac{\pi^2}{8t^2} + \left(1 - \frac{2}{\pi}\right)\frac{\lambda_g}{a} t^2, \tag{5.19}$$

where the first two terms come from expansion of $1/\sin\Theta(t)$. According to Eq. (5.19), $R_{T,\mathrm{eff}}(t)$ first decreases with t up to $t \sim (a/\lambda_g)^{1/4}$ and then starts to increase. This increase is a qualitatively new feature appearing due to the interaction. At the upper boundary of applicability of Eq. (5.17), at $t \sim a/\lambda_g$, one has $R_{T,\mathrm{eff}}(t)/R_T \sim a/\lambda_g \gg 1$. Thus, even within the range where the first correction is still small, weak Cooper repulsion changes the dependence of the effective interface resistance which starts to grow with the increase of t. The behavior of $R_{T,\mathrm{eff}}(t)$ at $t \geqslant a/\lambda_g$ will be studied in Sec. V C 3.

2. Strong repulsion

If the Cooper interaction is strong in the sense that

$$\lambda_g \gg a \equiv \frac{G_T}{4\pi g}, \tag{5.20}$$

then the initial stage of the evolution of $u(x)$ is better represented in terms of the RG equations for the coefficients γ_1 and γ_2 [cf. Eqs. (3.7) and (5.7)]:

$$\frac{d\gamma_1}{d\zeta} = -\lambda(\zeta)\gamma_1, \quad \frac{d\gamma_2}{d\zeta} = -\frac{1}{4}\gamma_1^2, \tag{5.21}$$

where $\lambda(\zeta)$ is given by Eq. (5.9). Simple calculation gives

$$\gamma_1(\zeta) = \frac{a\lambda_g}{\lambda_g \cosh\lambda_g\zeta + \lambda_d \sinh\lambda_g\zeta}, \tag{5.22a}$$

$$\gamma_2(\zeta) = -\frac{a^2/4}{\lambda_g \coth\lambda_g\zeta + \lambda_d}. \tag{5.22b}$$

At $\zeta \gg \zeta_1 \equiv \lambda_g^{-1}$, the first harmonics γ_1 vanishes, while the second one saturates at $\gamma_2^{(1)} = -a^2/4(\lambda_d + \lambda_g)$. The corresponding subgap conductance is then given by

$$G_A^{(1)} = -16\pi g \gamma_2^{(1)} = \frac{G_T^2}{4\pi g(\lambda_d + \lambda_g)}. \tag{5.23}$$

At the scale $\zeta \geqslant \zeta_1$ higher harmonics $\gamma_{n>2}$ are still much smaller than γ_2 once the condition (5.20) is fulfilled, so that

$$u(x) = -\tilde{a}\sin 2x, \quad \tilde{a} = \frac{a^2}{2(\lambda_d + \lambda_g)}. \tag{5.24}$$

From now on further evolution of $u(x,\zeta)$ with the increase of ζ is given by the solution of the Euler equation (3.10) with the initial condition (5.24) (a somewhat similar situation will be discussed in Sec. VI A). A change of variables $u(x,\zeta) = v(y,\eta)$ with $y = 2x - \pi$ and $\eta = 2\zeta$ makes the solution for $v(y,\eta)$ identical (up to the replacement $a \to \tilde{a}$) to the solution for $u(x,\zeta)$ discussed in Sec. III B. In particular, the ''shock wave'' develops in the solution for $u(x)$ at the scale $\zeta_2 = 1/2\tilde{a} = (\lambda_g + \lambda_d)/a^2$ that is much larger than ζ_1 under the condition (5.20).

To find the subgap conductance of the system with $\ln(L/d) \gg \zeta_1$, one should calculate, according to the general rule (4.14), the quantity $u_x(\pi/2,\zeta)$ with $\zeta = 2\ln(L/d)$. This calculation is simplified by the fact that $u(\pi/2,\zeta) \simeq 0$ at $\zeta \gg \zeta_1$. A similar situation was encountered in Sec. IV A where the normal-state conductance was considered. Differentiating Eq. (5.8) over x at $x = \pi/2$ under the condition $u(\pi/2) = 0$, one gets for the Andreev conductance $\partial G_A^{-1}/\partial\zeta = 1/4\pi g$, with the initial condition (5.23). As a result, one obtains

$$\frac{1}{G_A} \approx \frac{1}{G_A^{(1)}} + \frac{1}{2\pi g} \ln \frac{L}{d}, \tag{5.25}$$

where the first term is defined by Eq. (5.23), and the second term (which can be of arbitrary magnitude compared to the first one) is the normal-state resistance of the film (in units of $\hbar/e^2$). The first term in Eq. (5.25) has the meaning of the effective interface resistance defined in Eq. (4.18). In the leading order over λ_g/a, $R_{T,\mathrm{eff}}$ is given by $1/G_A^{(1)}$. Retaining also the next-to-leading contribution, one can write $R_{T,\mathrm{eff}}$ as

$$\frac{e^2}{\hbar} R_{T,\mathrm{eff}} = \frac{4\pi g(\lambda_g + \lambda_d)}{G_T^2} - \frac{C(\lambda_d/\lambda_g)}{\sqrt{g}} + O\left(\frac{G_T^2}{g^{3/2}}\right), \tag{5.26}$$

where the function $C(\lambda_d/\lambda_g)$ is of the order of 1 for $\lambda_d \sim \lambda_g$. The second term on the RHS of Eq. (5.26) is small compared to both terms in Eq. (5.25) once the conditions (5.20) and $\ln(L/d) \gg \zeta_1$ are fulfilled.

3. Effect of weak repulsion at large scales

Here we study the solution of the FRG equation (5.8) in the limit of weak repulsion. For the sake of simplicity we will consider the case of scale-independent $\lambda(\zeta) = \mathrm{const}$ corresponding to Finkelstein's fixed point $\lambda = \lambda_g$.

Consider first the qualitative effect of weak repulsion, $\lambda_g \ll a$, on the evolution of the function $u(x)$. At small $t \ll a/\lambda_g$, it leads to a small reduction of the amplitude of the solution compared to the noninteracting case. At $t \sim a/\lambda_g \gg 1$, when this correction becomes of the order of the solution itself, $u(x)$ changes its sign and becomes negative on some part of the interval $0 < x < \pi/2$. For even larger $t \gg a/\lambda_g$, $u(\pi/2)$ quickly approaches zero so that $u(x < \pi/2) < 0$ and $u(x > \pi/2) > 0$. Then the characteristics (5.11) with $x > \pi/2$ keep moving to the right, while the characteristics with $x < \pi/2$ move to the left, to the direction of negative x. As a result, a shock wave will appear also at $x = 0$, which, however, does not influence any physical results given by the derivatives of $u(x)$ at $x = \pi/2$. The numerical solution for $\lambda(\zeta) = \lambda_g = a/2$ is shown in Fig. 7.

To analyze Eq. (5.8) in the limit $\lambda_g \ll a$, it is convenient to make the following rescaling:

$$s = \lambda_g \zeta, \quad v = u/\lambda_g. \tag{5.27}$$

Then, in terms of the function $v(x,s)$, Eq. (5.8) takes the form

$$v_s + v v_x = -v(\pi/2)\sin x, \tag{5.28}$$

with the initial condition $v_0(x) = (a/\lambda_g)\sin x$.

Since the magnitude of this initial condition is much larger than 1, $v(x,s)$ acquires a sawlike behavior at $s \sim \lambda_g/a \ll 1$ (i.e., at $t \sim 1$). Therefore, the details of $v_0(x)$ are irrelevant for the study of the solution at large scales, $s \sim 1$, and one can formally consider the initial condition $v_0(x) = Ax$ with $A \to \infty$. The solution for Eq. (5.28) obtained with such $v_0(x)$ does not depend on λ_g and describes a universal behavior of the system for $t \gg 1$ in the limit of weak repulsion. The corresponding dependence $\Upsilon(s) = R_{T,\mathrm{eff}}(s)/R_D$ of the effective interface resistance obtained by numerical solution of Eq. (5.28) and normalized to R_D is shown in Fig. 8. The function $\Upsilon(s)$ has a maximum $\Upsilon = 0.406$ at $s = 1.95$, and in the limiting cases it is given by

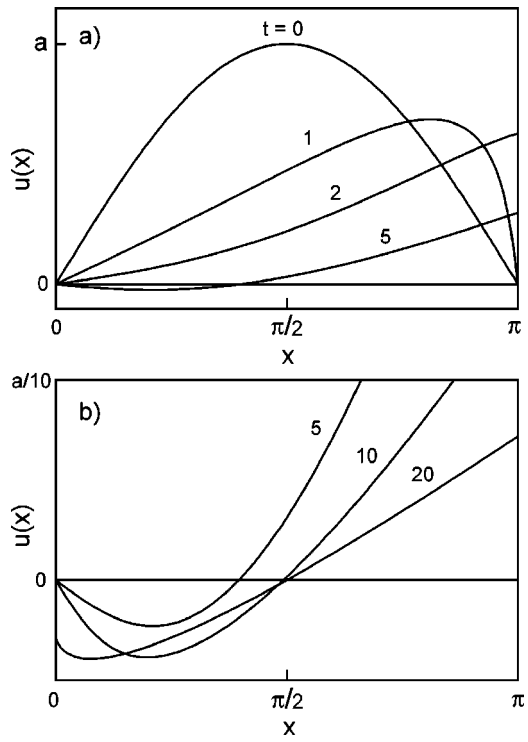

FIG. 7. Solutions for Eq. (5.8) with $\lambda/a = 1/2$ for different values of t: (a) initial stage of evolution, (b) solution for large t.

$$\Upsilon(s) = \begin{cases} (1 - 2/\pi)s, & \text{for } s \ll 1, \\ 1.19/s, & \text{for } s \gg 1. \end{cases} \tag{5.29}$$

4. Arbitrary λ *and* t

Solution of the FRG equation (5.8) for arbitrary λ and t should be obtained numerically. The effective interface resistance $R_{T,\mathrm{eff}}$ normalized to the tunneling resistance R_T as a function of $t = R_D/R_T$ is plotted in Fig. 9 [as in Sec. V C 3,

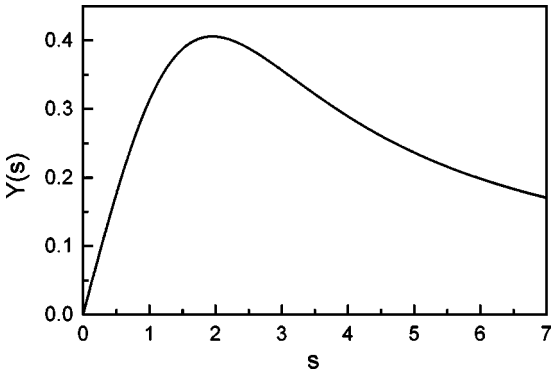

FIG. 8. The universal function $\Upsilon(s) = R_{T,\mathrm{eff}}/R_D$ vs $s = (\ln L/d)/\pi\sqrt{g}$.

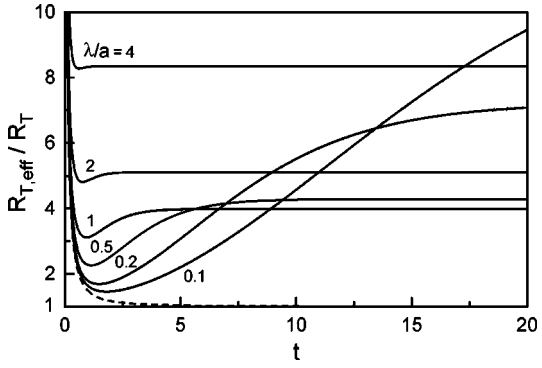

FIG. 9. Dependence of the effective interface resistance $R_{T,\mathrm{eff}}(t)/R_T$ vs $t=R_D/R_T$ for different values of λ/a obtained by numerical solution of Eq. (5.8) for $\lambda(\zeta)=\mathrm{const}$. The dashed line corresponds to the noninteracting case, $\lambda=0$.

we consider $\lambda(\zeta)=\lambda_g=\mathrm{const}$]. The dashed line shows $R_{T,\mathrm{eff}}/R_T=1/\sin\Theta(t)$ for the noninteracting case [cf. Eq. (4.17)].

For the case of strong repulsion, $\lambda_g\gg a$, $R_{T,\mathrm{eff}}(t)$ very quickly (at $t\sim a/\lambda_g\ll 1$) reaches its asymptotic value and saturates at $R_{T,\mathrm{eff}}(t=\infty)\approx(2\lambda_g/a)R_T$; cf. Eq. (5.26). The limiting value $R_{T,\mathrm{eff}}(\infty)$ decreases with the decrease of λ_g/a up to $\lambda_g/a\sim 1$. For small λ_g/a, corresponding to the case of weak repulsion, it starts to grow again with $R_{T,\mathrm{eff}}(\infty)/R_T\approx 1.19a/\lambda_g$, according to Eq. (5.29). Note that in this limit $R_{T,\mathrm{eff}}(t)$ reaches its asymptotic value at large scale $t\sim a/\lambda_g$. The dependence of $R_{T,\mathrm{eff}}(\infty)$ as a function of λ_g/a is shown in Fig. 10.

The most striking feature of Fig. 9 is a nonmonotonous dependence of $R_{T,\mathrm{eff}}(t)$, especially pronounced for weak repulsion, $\lambda_g\ll a$. In this limit, the effective interface resistance significantly exceeds its noninterating value R_T at large scales $t\gg(a/\lambda_g)^{1/2}$. Such a nonmonotonous dependence arises even within applicability of the first-order correction (5.17) as discussed at the end of Sec. V C 1. Another important feature of Fig. 9 is that the limits $\lambda\to 0$ and $R_D\to\infty$ *do not commute*. Indeed, for any small but finite λ_g, $R_{T,\mathrm{eff}}(t)/R_T$ will eventually (though at very large t) deviate from the noninteracting dependence (dashed line in Fig. 9) and become large.

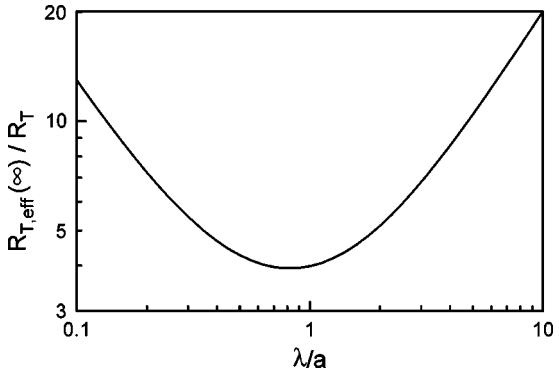

FIG. 10. The limiting value $R_{T,\mathrm{eff}}(t=\infty)/R_T$ vs λ/a [for $\lambda(\zeta)=\mathrm{const}$].

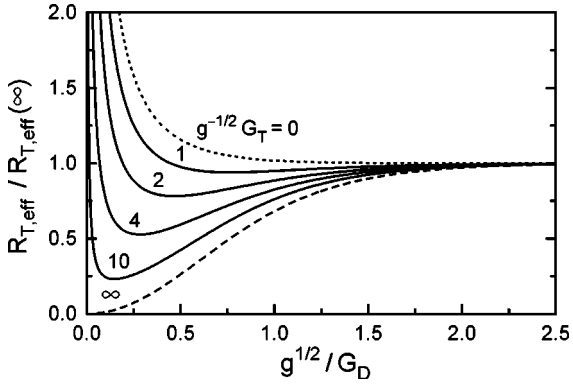

FIG. 11. The effective interface resistance $R_{T,\mathrm{eff}}$ normalized to its limiting value at $G_D^{-1}=\infty$ (see Fig. 10) as a function of $\sqrt{g}/G_D=\lambda_g\zeta/2$ for various values of $G_T/\sqrt{g}$. The plot corresponds to Finkelstein's fixed point $\lambda=\lambda_g\equiv 1/(2\pi\sqrt{g})$.

We will see in Sec. VI that such a nonmonotonous dependence of $R_{T,\mathrm{eff}}(t)$ will manifest itself in a nonmonotonous temperature and voltage behavior of the subgap conductance.

In this section we assumed that $\lambda(\zeta)$ had already reached its fixed-point value $\lambda_g=1/(2\pi\sqrt{g})$, so that $\lambda_g/a=2\sqrt{g}/G_T$. Thus, the limits of strong and weak interactions are separated by $G_T\sim\sqrt{g}$. For $G_T\ll\sqrt{g}$, the interaction is strong, and for $G_T\gg\sqrt{g}$ (and, in particular, for the case of a completely transparent interface, $G_T=\infty$), the interaction is weak. It is then natural to measure all dimensionless conductances in units of $\sqrt{g}$. The effective interface resistance $R_{T,\mathrm{eff}}$ normalized to its limiting value $R_{T,\mathrm{eff}}(\infty)$ at large spatial scales (cf. Fig. 10) as a function of $\sqrt{g}/G_D=s/2=\lambda_g\zeta/2$ is shown in Fig. 11, with different curves corresponding to different values of $G_T/\sqrt{g}$. The asymptotic curve (dashed line) for the transparent interface, $G_T\to\infty$, is given by $R_{T,\mathrm{eff}}=\Upsilon[2\sqrt{g}(e^2R_D/\hbar)]R_D$; cf. Eq. (5.29). In this limit, for $R_D\gg\hbar/e^2\sqrt{g}$ one has

$$\frac{e^2}{\hbar}R_A=\frac{0.6}{\sqrt{g}}+\frac{1}{2\pi g}\ln\frac{L}{d}. \tag{5.30}$$

D. Noise

In this section we will analyze the effect of interaction on the noise of N-S current. As shown in Sec. IV C, the current-current correlator is determined by the noise function $P_S(t)$; see Eqs. (4.19) and (4.20). Qualitatively, P_S can be estimated by comparing the effective tunneling resistance $R_{T,\mathrm{eff}}$ with the diffusive resistance R_D. If $R_{T,\mathrm{eff}}\gg R_D$, then $P_S\approx 3$, while in the opposite case ($R_{T,\mathrm{eff}}\ll R_D$) $P_S\approx 1$. As in Sec. V C 3, we will assume here that the $\lambda(\zeta)$ has already reached its fixed point $\lambda=\lambda_g$. Then P_S becomes a function of two parameters $t=R_D/R_T$ and $\lambda_g/a=2\sqrt{g}/G_T$. Summarizing results of Sec. V C, one can sketch the boundaries between regions with $P_S=3$ and $P_S=1$ on the plane $(\log t,\log(G_T/\sqrt{g}))$; see Fig. 12.

In the case of strong repulsion $G_T\ll\sqrt{g}$, the function $u(x)$ very quickly (at $t\sim G_T/\sqrt{g}$) reduces to the second harmonic, Eq. (5.24), and $R_{T,\mathrm{eff}}$ saturates at $R_{T,\mathrm{eff}}=R_A^{(1)}$

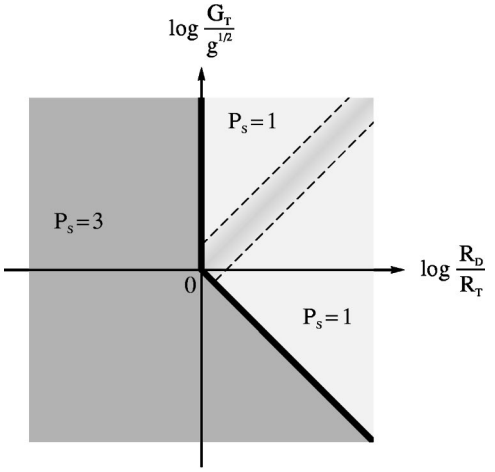

FIG. 12. Schematic map of the noise coefficient P_S as a function of the tunnel and diffusive resistances in the presence of Cooper repulsion $\lambda=\lambda_g$. The dark area refers to the tunnel limit $P_S\approx 3$, whereas light regions correspond to the diffusive regime with $P_S \approx 1$.

$\equiv(4\sqrt{g}/G_T)R_T$ [cf. Eq. (5.23)]. As explained in Sec. V C 2, further evolution of $u(x)$ is analogous (after a proper rescaling and shift of variables) to the evolution of $u(x)$ for the noninteracting case considered in Sec. III B. The property $u(\pi/2)=0$ makes the calculation of the noise function P_S analogous to the calculation of the function P_N for the case of the *normal* island; see Sec. IV A. So one obtains $P_S^{\rm int}=P_N(R_D/R_A^{(1)})$. Thus, in the limit $G_T \ll \sqrt{g}$, the crossover between the tunnel ($P_S=3$) and diffusive ($P_S=1$) character of noise is shifted to $t\sim\sqrt{g}/G_T \gg 1$; see Fig. 12.

In the limit of weak repulsion, $G_T \gg \sqrt{g}$, the situation is more interesting. For $t\sim 1$, interaction corrections can be neglected and P_S is given by the noninteracting expression (4.22). So, at $t\sim 1$, P_S decreases from 3 to 1, the corresponding boundary being shown in Fig. 12. Later, at $t\sim G_T/\sqrt{g} \gg 1$ (when $R_D\sim\hbar/e^2\sqrt{g}$) interaction corrections become relevant. In this region, $R_{T,\rm eff}$ is of the order of R_D (cf. Fig. 8), and one may anticipate that P_S will deviate from 1. For even larger t when the resistance is dominated by the diffusive conductor, P_S will eventually reduce to 1. This crossover region is marked in Fig. 12 by the dashed lines.

The behavior of P_S in the crossover region $t\sim G_T/\sqrt{g} \gg 1$ can be obtained by numerical solution of Eq. (5.28). The resulting $P_S(s)$ is plotted as a function of $s=\lambda_g\zeta=(\ln L/d)/\pi\sqrt{g}=2(e^2/\hbar)R_D\sqrt{g}$ [cf. Eq. (5.27)] in Fig. 13. $P_S(s)$ has a minimum $P_S=0.99$ at $s=0.40$ and a maximum $P_S=1.28$ at $s=3.25$.

The negative derivative of $P_S(s)$ for $s\ll 1$ can be obtained analytically. Seeking the solution of Eq. (5.28) as a series over s, one finds

$$v(x,s)=\frac{x}{s}-\frac{\pi(1-\cos x)}{2x}+O(s), \qquad (5.31)$$

where the first term is the usual saw function, while the other terms are due to the RHS of Eq. (5.28). Now, with the help of Eq. (4.20) one gets for $s\ll 1$

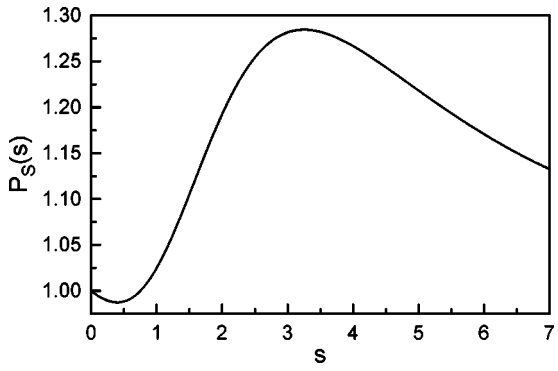

FIG. 13. Noise function $P_S(s)$ vs $s=2\sqrt{g}/G_D$ for the case of weak interaction, $G_T \gg \sqrt{g}$.

$$P_S(s)=1-\left(\frac{1}{2}-\frac{12}{\pi^2}+\frac{24}{\pi^3}\right)s=1-0.058\ s. \qquad (5.32)$$

VI. TEMPERATURE, VOLTAGE, AND MAGNETIC FIELD EFFECTS

A. General analysis

In this section we consider the case of a superconductive island in the situation when temperature and/or voltage are high compared to the Thouless energy or the perpendicular magnetic length $l_H=\sqrt{\Phi_0/H}$ is shorter than the system size L. Then Cooperon coherence is destroyed at the energy scale $\Omega_*>E_{\rm Th}$, where $\Omega_*=\max(T,eV,eDH/c)$. At the same time we will assume that the frequency ω of the external voltage (or current) is smaller than the Thouless energy.

According to the general approach explained in Sec. III C, we have to determine an effective proximity action via the RG procedure accomplished down to the energy scale $E_{\rm Th}$. Now the whole energy interval of the RG, $\omega_d>\Omega>E_{\rm Th}$, can be divided into two regions with different FRG equations. In the region $\omega_d>\Omega>\Omega_*$, renormalization of the action (3.1) is described by Eq. (3.10) derived in Sec. III for the noninteracting case or its analog (5.8) in the presence of an interaction. In the region $\Omega_*>\Omega>E_{\rm Th}$, Cooperons are suppressed while diffuson modes still contribute to the renormalization of the action (3.1). Thus, at large scales, $\Omega<\Omega_*$, the charges γ_n depend on two RG ''time'' arguments ζ and $\zeta_*\equiv\ln(\omega_d/\Omega_*)$. For $\zeta>\zeta_*$, the bulk matrix Q is purely diagonal in Nambu space [cf. Eq. (2.3)]. On the other hand, according to Eq. (2.8), the island's matrix Q_S is off diagonal in Nambu space, due to the Andreev nature of the subgap tunneling across the interface. As a result, $\mathrm{tr}(Q_SQ)^n$ with odd n vanishes, and so γ_n's with odd n do not contribute to the multicharge RG equation (3.7) at scales $\zeta>\zeta_*$.

To describe the evolution of γ_n's at $\zeta>\zeta_*$, one should modify the derivation presented in Sec. III B for the case of even n. The difference is that now only the first line of Eq. (A2) corresponding to diffuson pairing contributes to the average $\Delta S_{k,n}=i\langle S_{{\rm int},k}S_{{\rm int},n}\rangle$. But for even k and n, and at $\zeta>\zeta_*$, the matrices A and B defined in Eq. (3.4) commute with τ_z. Then the zero-energy limit of the first line of Eq. (A2) reproduces Eq. (A3) used in the derivation of Eq. (3.5).

Hence, we conclude that evolution of $\{\gamma_{2m}\}$ at $\zeta>\zeta_*$ is described by the same Eq. (3.7), with all γ_{2m+1} set to zero.

To describe evolution of the set $\{\gamma_n\}$ at $\zeta>\zeta_*$, we find it convenient to introduce Fourier transformation with respect to even n:

$$\tilde{u}(x)=\sum_{n=1}^{\infty} 2n\gamma_{2n}\sin 2nx=\frac{1}{2}[u(x)-u(\pi-x)]. \quad (6.1)$$

Then the FRG equation for the function $\tilde{u}(x)$ acquires the form of the Euler equation:

$$\tilde{u}_\zeta+\tilde{u}\tilde{u}_x=0. \quad (6.2)$$

The function $\tilde{u}(x,\zeta;\zeta_*)$ that determines physical quantities (see below) is then given by the solution of Eq. (6.2) with the initial condition

$$\tilde{u}(x,\zeta_*;\zeta_*)=\frac{1}{2}[u(x,\zeta_*)-u(\pi-x,\zeta_*)], \quad (6.3)$$

where $u(x,\zeta_*)$ is the solution for the FRG equation (5.8) at $\zeta_*=\ln(\omega_d/\Omega_*)$. We want to emphasize that the reduction $u(x)\to\tilde{u}(x)$ at $\zeta=\zeta_*$ describes the crossover from the $\Omega_*\ll E_{\rm Th}$ to $\Omega_*\gg E_{\rm Th}$ regimes only with logarithmic accuracy. The number in the correct cutoff of logarithm is beyond the RG precision.

Below we apply the described scheme to the calculation of physical quantities. To determine the Andreev conductance at large $\Omega_*>E_{\rm Th}$ in terms of the function $\tilde{u}(x)$ we should use a generalized version of Eq. (4.13). Namely, we should take into account that for $\epsilon>E_{\rm Th}$, parameters γ_{2n} depend on the energy argument ϵ running under the trace [cf. Eq. (B3)], since it is just the value of ϵ which determines the Cooperon coherence scale. Thus, $\gamma_{2n}(\epsilon)$ should be put under the sign of Tr in Eq. (4.13). The trace operator contains an integral over ϵ those main contribution comes from $\epsilon\sim\Omega_*$. As a result, we obtain the following expression for the (nonlinear) current:

$$I(V)=\frac{e^2}{\hbar}G_A(\Omega_*)V, \quad (6.4)$$

where the value of $G_A(\Omega_*)$ is determined to logarithmic accuracy as

$$G_A(\Omega_*)\equiv G_A(t,t_*)=4\pi g\tilde{u}_x\left(\frac{\pi}{2},\zeta;\zeta_*\right). \quad (6.5)$$

Calculation of $\tilde{u}_x(\pi/2)$ is very simple since $\tilde{u}(\pi/2)=0$:

$$\left.\frac{\partial(1/G_A)}{\partial\zeta}\right|_{\zeta>\zeta_*}=\frac{1}{4\pi g}; \quad (6.6)$$

cf. the normal-metal case discussed in Sec. IV A.

Equations (6.5) and (6.6) can be naturally interpreted with the help of the effective interface resistance $R_{T,\rm eff}$ introduced in Eq. (4.18). An important property of this quantity is that it is formed by Cooperons only which are taken into account by the FRG equation for $u(x)$. At scales $t>t_*\equiv a\zeta_*$, Cooperon coherence is lost, and $R_{T,\rm eff}(t)$ saturates at the constant level $R_{T,\rm eff}(t_*)$, becoming independent of R_D anymore. As a result,

$$R_A(t,t_*)=R_D+R_{T,\rm eff}(t_*), \quad (6.7)$$

where $R_D=R_T t=\ln(L/d)/2\pi\sigma$ is the energy-independent resistance of the normal film.

Considerations that lead to Eq. (6.5) can be generalized to higher correlators of current as well. To logarithmic accuracy, the noise power is given by the zero-energy expressions (4.19) and (4.20) with $u(x,\zeta)$ replaced by $\tilde{u}(x,\zeta;\zeta_*)$. The quantities $\tilde{u}_x(\pi/2)$ and $\tilde{u}_{xxx}(\pi/2)$ entering this expression can be calculated similarly to Eq. (4.9):

$$\tilde{u}_x\left(\frac{\pi}{2},\zeta;\zeta_*\right)=\frac{u_x(\pi/2,\zeta_*)}{1+(\zeta-\zeta_*)u_x(\pi/2,\zeta_*)}, \quad (6.8)$$

$$\tilde{u}_{xxx}\left(\frac{\pi}{2},\zeta;\zeta_*\right)=\frac{u_{xxx}(\pi/2,\zeta_*)}{[1+(\zeta-\zeta_*)u_x(\pi/2,\zeta_*)]^4}. \quad (6.9)$$

As a result, the current-current correlation function can be written in the form similar to Eq. (4.19):

$$\langle I_\omega I_{-\omega}\rangle=\frac{e^2G_A(t,t_*)}{3\hbar}\left\{[3-P_S(t,t_*)]\Psi(\omega)+\frac{1}{2}P_S(t,t_*)\right.$$
$$\left.\times[\Psi(\omega-2eV)+\Psi(\omega+2eV)]\right\}, \quad (6.10)$$

where $G_A(t,t_*)$ is given by Eq. (6.7), and the noise function $P_S(t,t_*)$ depends now on two RG ''time'' variables. Using Eqs. (4.14), (4.20), (6.5), and (6.7), one obtains

$$P_S(t,t_*)=1+\frac{G_A^3(t,t_*)}{G_A^3(t_*,t_*)}[P_S(t_*)-1]. \quad (6.11)$$

Here both $G_A(t_*,t_*)\equiv G_A(t_*)$ and $P_S(t_*)$ are given by the zero-energy results at $t=t_*$.

B. Noninteracting case

1. Andreev conductance

To calculate the Andreev conductance we substitute $R_{T,\rm eff}(t_*)=R_T/\sin\Theta(t_*)$ into Eq. (4.18):

$$G_A(\Omega_*)=G_T\frac{\sin\Theta(t_*)}{1+t\sin\Theta(t_*)}=G_D\frac{t\sin\Theta(t_*)}{1+t\sin\Theta(t_*)}, \quad (6.12)$$

which can be obtained from the zero-energy result (4.17) by the replacement $\Theta(t)\to\Theta(t_*)$.

Below we apply Eq. (6.12) to the analysis of two specific examples.

We start from the case of the *linear* conductance as a function of temperature. The corresponding curves $G_A(T)$ for several values of the ratio $t=G_T/G_D$ are presented in Fig. 14. In the limit $G_T\gg G_D$ any dependence on T disappears and N-S conductance is equal to the diffusive conductance G_D. This result is in disagreement with

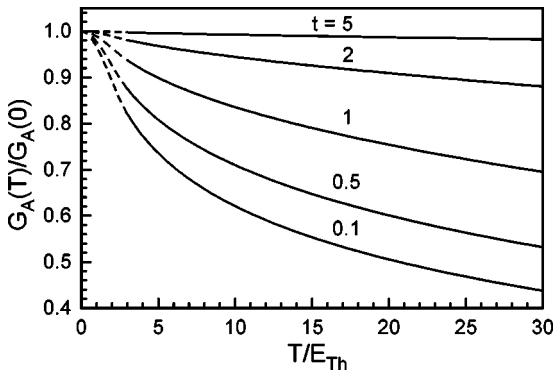

FIG. 14. The linear Andreev conductance $G_A(T)$ normalized to its zero-temperature value vs $T/E_{\rm Th}$ for different values of the ratio $t=G_T/G_D$. The plot corresponds to the geometry shown in Fig. 1 with $L/d=20$, i.e., $\omega_d/E_{\rm Th}=400$. In the intermediate region $T\sim E_{\rm Th}$ (sketched by a dashed line), corrections are nonlogarithmic and cannot be taken into account within the RG approach.

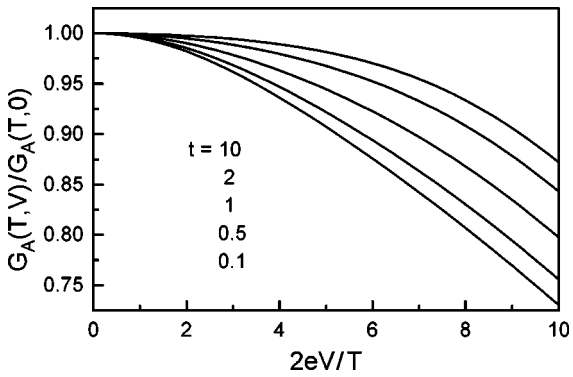

FIG. 15. The nonlinear Andreev conductance $G_A(T,V)$ normalized to the linear conductance $G_A(T,0)$ vs the ratio $2eV/T$ for $T/E_{\rm Th}=10$. As in Fig. 14, $\omega_d/E_{\rm Th}=400$. Different curves correspond to different ratios $t=G_T/G_D$: 0.1 (bottom), 0.5, 1, 2, 10 (top).

calculations[35,17] which predict, for an ideal N-S structure in the 1D geometry, a conductance maximum at $T\sim E_{\rm Th}$ with the relative magnitude about 10% (the so-called finite-bias anomaly). This discrepancy is due to the limited precision of our calculation scheme, which is equivalent to the summation of the main logarithmic terms. The finite-bias anomaly is due to the energy dependence of the effective diffusion constant $D(\epsilon)$ at $\epsilon\sim E_{\rm Th}$, and this effect is beyond the main logarithmic approximation. As one can see from Fig. 14, the zero-bias anomaly is stronger than the finite-bias anomaly for small enough values of t.

Consider now the *nonlinear* subgap conductance at high temperature $T\gg E_{\rm Th}$ and arbitrary relation between T and eV. At $eV\ll T$ we are back to the linear conductance case with $t_*=t_T\equiv(G_T/4\pi g)\ln(\omega_d/T)$, whereas at large voltage $eV\gg T$ we have $t_*=t_V\equiv(G_T/4\pi g)\ln(\omega_d/eV)$.

To find the behavior of $G_A(T,V)$ in the crossover region $eV\sim T\gg E_{\rm Th}$ we need to improve the logarithmic accuracy of Eq. (6.12). To this end, we perform a more accurate calculation of the energy integral under the trace in the generalized version of Eq. (4.13) taking into account the energy dependence of $\gamma_n(E)$:

$$\frac{G_A(T,V)}{G_D}=\frac{1}{2eV}\int_0^\infty dE\left[\tanh\frac{E_+}{2T}-\tanh\frac{E_-}{2T}\right]\times\frac{t\sin\Theta(t_E)}{1+t\sin\Theta(t_E)},\tag{6.13}$$

where $E_\pm=E\pm eV$ and $t_E=(G_T/4\pi g)\ln(\omega_d/E)$. The logarithmic factor $\ln(\omega_d/E)$ comes from the integration over 2D Cooperon modes, $\int^{1/d}d^2\mathbf{q}/(Dq^2\pm 2iE)$, which determines the Cooperon amplitude at coinciding point (i.e., the probability of return). In the presence of a transverse magnetic field, Cooperon modes are quantized, so integration over momenta is substituted by the summation over Landau levels; see, e.g., Ref. 36. Then the effect of magnetic field upon the subgap conductance can be accounted by the replacement of t_E in Eq. (6.13) by

$$t_E(H)=\frac{G_T}{4\pi g}\left[\ln\frac{\hbar c}{2eHd^2}-\mathrm{Re}\,\psi\left(\frac{1}{2}-i\frac{Ec}{2eDH}\right)\right],\tag{6.14}$$

where $\psi(x)=d\ln\Gamma(x)/dx$ is the digamma function.

In the limiting case of weak interface transparency, $t\ll 1$, the Andreev conductance is given by

$$\frac{G_A(T,V,H)}{G_T^2/4\pi g}=\begin{cases}\ln\dfrac{\omega_d}{eV}+1, & \text{for } eV\gg\left(T,\dfrac{eDH}{c}\right),\\ \ln\dfrac{2\omega_d}{\pi T}+\gamma, & \text{for } T\gg\left(eV,\dfrac{eDH}{c}\right),\\ \ln\dfrac{2\omega_d c}{eDH}+\gamma, & \text{for } \dfrac{eDH}{c}\gg(T,eV),\end{cases}\tag{6.15}$$

where $\gamma=0.577\ldots$ is the Euler constant. Comparing these asymptotics, we conclude that a crossover from the voltage to temperature-dominated effective interface resistance occurs at $2eV\approx\pi e^{1-\gamma}T\approx 4.8T$. Similarly, a crossover from the temperature- to magnetic-field-dominated resistance occurs at $H\approx\pi cT/eD$.

For arbitrary t, the behavior of G_A in the crossover region should be obtained by numerical integration in Eq. (6.13). The corresponding plots of $G_A(T,V)$ as a function of $2eV/T$ for different values of t are presented in Fig. 15. Note, finally, that the difference between the nonlinear conductance $G_A(V)\equiv I_A/V$ and the differential conductance dI_A/dV should be neglected in the main logarithmic approximation.

2. Current fluctuations

In order to calculate the noise function $P_S(t,t_*)$ at $\Omega_*\gg E_{\rm Th}$ we substitute Eqs. (4.22) and (6.12) into Eq. (6.11). As a result, we obtain

$$P_S(t,t_*)=1+\frac{1+\Theta_*\tan\Theta_*+3\Theta_*\cot\Theta_*}{2(1+\Theta_*\tan\Theta_*)(1+t\sin\Theta_*)^3},\tag{6.16}$$

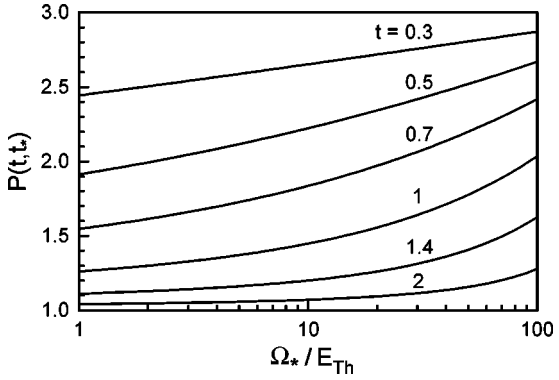

FIG. 16. Noise function $P_S(t,t_*)$ vs $\Omega_*/E_{\rm Th}$ for different values of $t=G_T/G_D$. As in Fig. 14, the ratio $\omega_d/E_{\rm Th}=400$.

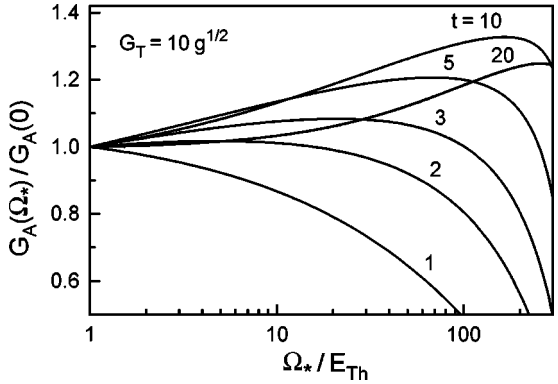

FIG. 17. Dependence of the Andreev conductance $G_A(\Omega_*)$ (normalized to the zero-energy value) on the ratio $\Omega_*/E_{\rm Th}$ for different values of *t*. For all plots, $\omega_d/E_{\rm Th}=400$, $\lambda=\lambda_g$, and $G_T=10\sqrt{g}$.

where $\Theta\equiv\Theta(t)$, $\Theta_*\equiv\Theta(t_*)$, and $G_A(\Omega_*)$ is given by Eq. (6.5).

Equations (6.10) and (6.16) determine fluctuations of N-S current as a function of temperature, voltage, magnetic field, and frequency ($\omega\ll E_{\rm Th}$) at arbitrary values of the ratio $t=G_T/G_D$. The dependence of noise upon *T*, *V*, and ω comes in two different ways: via the functions $\Psi(\omega\pm 2eV)=\Omega\coth[(\omega\pm 2eV)/2T]$ and via the Cooperon cutoff scale $\Omega_*=\max(T,eV,\omega,eDH/c)$ which determines $t_*=(G_T/4\pi g)\ln(\omega_d/\Omega_*)$. In the limit $t\to\infty$, the function $P_S(t,t_*)/3$ approaches 1/3 and the expression for noise reduces to the standard form[19] for purely diffusive N-S junction at $\Omega_*<E_{\rm Th}$.[37] However, the range of *t* where such a universal behavior sets in does depend upon Ω_*: the increase of Ω_* leads to the decrease of the proximity angle Θ_*, which, in turn, increases the factor $P_S(t,t_*)$. A number of curves characterizing the behavior of $P_S(t,t_*)$ as a function of $\Omega_*/E_{\rm Th}$ at different values of *t* are presented in Fig. 16.

C. Effects of interaction

This section contains the main application of our theory since variation of temperature, voltage, or magnetic field is a natural tool to study system properties. Here all effects discussed in the body of the paper come into play altogether. Therefore, we will repeat briefly the main concepts the reader could gain from the above discussion.

At scales smaller than the Cooperon coherence length $\sqrt{D/\Omega_*}$, i.e., at $\zeta<\zeta_*\equiv\ln(\omega_d/\Omega_*)$, the system is described by the function $u(x,\zeta)$ which evolves according to the FRG equation (5.8). At larger scales, $\zeta>\zeta_*$, one should introduce a ''two-time'' function $\tilde{u}(x,\zeta;\zeta_*)$. It is obtained from $u(x,\zeta)$ by the reduction (6.3) and obeys the FRG equation (6.2). The conductance and noise power are given by Eqs. (4.14) and (4.20), with $u(x,\zeta)$ being substituted by $\tilde{u}(x,\zeta;\zeta_*)$ and $\zeta=\ln(\omega_d/E_{\rm Th})=2\ln(L/d)$. The Ω_* dependence of the conductance can be easily expressed with the help of the effective interface resistance according to Eq. (6.7).

In the noninteracting approximation the effect of large $\Omega_*\gg E_{\rm Th}$ was to decrease the Andreev conductance compared to the zero-energy limit, $\Omega_*\ll E_{\rm Th}$, due to the increase of $R_{T,\rm eff}(t_*)$. The drastic change introduced by the Cooper interaction is that $R_{T,\rm eff}(t_*)$ shown in Fig. 9 is no longer a monotonous function of t_*. Therefore, depending on the relation between parameters of the problem, the subgap conductance may either decrease or increase with the increase of Ω_*. This unusual enhancement of conductivity with the increase of the decoherence energy scale Ω_* is most pronounced in the limit of weak repulsion, $G_T\gg 2\sqrt{g}$ [we again assume that $\lambda(\zeta)$ had reached Finkelstein's fixed point λ_g]. In this case, according to the results of Sec. V C 1, $R_{T,\rm eff}(t_*)$ decreases with t_* at $t_*\ll(G_T/\sqrt{g})^{1/4}$ and increases with t_* at $t_*\gg(G_T/\sqrt{g})^{1/4}$; cf. Eq. (5.19). Hence, the total conductance decreases with the growth of Ω_* for $\Omega_*\gg\Omega_{\rm cr}$ and increases for $\Omega_*\ll\Omega_{\rm cr}$, where $\Omega_{\rm cr}=\omega_d\exp(-cg^{7/8}/G_T^{3/4})$ and $c=2\pi^{7/4}(\pi-2)^{-1/4}\approx 14.3$. Since the total resistance is the sum of $R_{T,\rm eff}$ and R_D [cf. Eq. (6.7)], the magnitude of the effect is determined by the ratio $R_{T,\rm eff}/R_D$ which, according to Fig. 8, has a maximum at $t\approx G_T/\sqrt{g}$. An example of such a nonmonotonous dependence of $G_A(\Omega_*)$ is shown in Fig. 17. The curves differ by the ratio $t=R_D/R_T$ and correspond to $G_T=10\sqrt{g}$ (i.e., $\lambda_g/a=0.2$).

In the opposite case of strong repulsion, $G_T\ll 2\sqrt{g}$, the Ω_* dependence of G_A is absent for $t_*\gg G_T/\sqrt{g}$ when $R_{T,\rm eff}(t_*)$ is t_* independent. The reason is that strong repulsion makes Cooperons ineffective at scales $\zeta\gg\zeta_1\equiv 1/\lambda_g$ when all γ_n's with odd *n* vanish; see Sec. V C 2. Therefore, the reduction $u(x)\to\tilde{u}(x)$ at the scale ζ_* leaves the function $u(x)$ intact, indicating that physical results are Ω_* independent. They become Ω_* dependent at relatively large scales when $\zeta_*<\zeta_1$, i.e., at $\ln(\omega_d/\Omega_*)<2\pi\sqrt{g}$. The principal effect of Ω_* is then to decrease G_A with the increase of Ω_*.

Finally, we will dwell on the Ω_* dependence of the noise power. According to Eq. (6.10), the latter is described by the function $P_S(t,t_*)$ which now depends on two RG ''time'' arguments. Equation (6.11) relates $P_S(t,t_*)$ to the zero-energy expressions for $G_A(t_*)$ and $P_S(t_*)$.

We start from the case of the weak interaction. The crossover from the tunnel ($P_S=3$) to diffusive ($P_S=1$) character of noise at $t,t_*\sim 1$ is well described within the noninteracting approximation investigated above. To study the noise

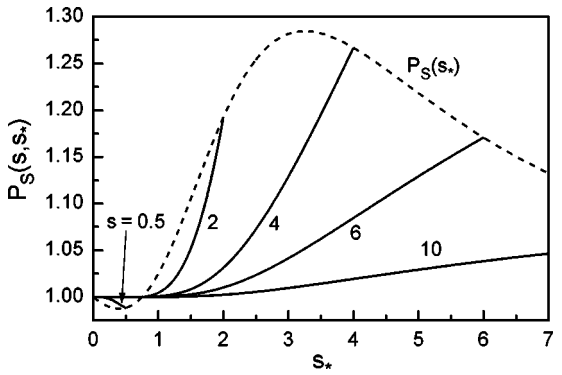

FIG. 18. Noise function $P_S(s,s_*)$ vs s_* for different values of s. The dashed line shows $P_S(s_*,s_*)=P_S(s_*)$.

function in the vicinity of the interaction-induced peak in P_S at $t,t_*\sim G_T/\sqrt{g}\gg 1$ (cf. Fig. 13) we substitute the functions $\Upsilon(s)$ and $P_S(s)$ shown in Figs. 8 and 13, respectively, into Eq. (6.11). The resulting dependence of $P_S(s,s_*)$ as a function of s_* is plotted in Fig. 18 for different values of s. We remind the reader that $P_S(s,s_*)$ is defined at $s_*<s$ and reduces to the zero-energy result at coincident ''times'': $P_S(s_*,s_*)=P_S(s_*)$. The latter function is sketched in Fig. 18 by the dashed line. Taking into account that $s_*=\lambda_g\zeta_*=(1/2\pi\sqrt{g})\ln(\omega_d/\Omega_*)$, one obtains from Fig. 18 that P_S decreases with the increase of the Cooperon decoherence energy scale Ω_* (at $t,t_*\gg 1$), as if the system becomes more diffusive. This trend is opposite to what one has in the noninteracting case when the increase of Ω_* drives the system toward the tunnel limit, thus increasing P_S. Note also that, contrary to $P_S(s)$ (cf. Fig. 13), $P_S(s,s_*)$ shown in Fig. 18 is a monotonous function of s_* at a fixed s.

In the limit of strong repulsion, $G_T\ll\sqrt{g}$, the zero-energy noise function $P_S(t)$ exhibits a crossover from the tunnel to diffusive regimes at $t\sim\sqrt{g}/G_T\gg 1$. Nevertheless, $P_S(t,t_*)$ remains t_* independent up to much smaller $t_*\sim G_T/\sqrt{g}\ll 1$ corresponding to relatively large energy scales $\ln(\omega_d/\Omega_*)\simeq 2\pi\sqrt{g}$. This effect is of the same origin as the above-mentioned Ω_* independence of G_A in the limit of strong repulsion.

VII. CONCLUSIONS

We have shown in this paper that electron transport through mesoscopic N-I-S structures can be fully described in terms of the Keldysh-space proximity action $S_{\rm prox}[Q_S,Q_N]$, as defined in Eq. (3.13). This action is a functional of two matrices Q_S and Q_N, corresponding to the superconductive and normal leads. Throughout the paper, we choose the gauge with the normal lead being in equilibrium, with $Q_N=\Lambda$. The superconductive terminal is characterized by the matrix Q_S which contains both the classical (φ_1) and quantum (φ_2) components of the order parameter phase. The physical response and correlation functions of any order can be determined from the proximity action by calculating the derivatives with respect to the quantum component at a given value of the classical component of the phase, as explained in the beginning of Sec. IV. In principle, the proximity action functional contains information about full charge transfer statistics (cf. Refs. 30, 31, and 33).

The proximity action functional is known once the set of ''charges'' γ_n or, equivalently, the periodic function $u(x)$, Eq. (3.9), is specified. It was explained in Sec. III C that the function $u(x)$ is directly related to the generating functional for the transmission coefficients, introduced in Ref. 4. Actually, the proximity action approach bears an obvious analogy with the scattering matrix approach[6,4] as both describe transport properties in terms of the characteristics of the terminals (stationary-state Green functions of the terminals $Q_{S,N}$ in the former versus asymptotic scattering states in the latter approach). The proximity action method is well suited for the treatment of interaction effects in the contact region; the task which is out of reach for the standard scattering-matrix technique.

Actual calculation of the function $u(x)$ that determines the proximity action is accomplished by the functional renormalization group method. In the simplest case (no interaction in the N region, and all relevant energies are much below the Thouless energy scale $E_{\rm Th}=\hbar D/L^2$) the FRG equation reduces to the Euler equation (3.10) for 1D motion of a compressible gas. Although we derived this equation for the normal conductor of 2D geometry, its solution, Eq. (3.12), is applicable (being expressed in terms of the ratio $t=G_T/G_D$ of the tunneling to diffusive conductances) to any coherent conductor. If higher-energy scales $\Omega\geqslant E_{\rm Th}$ or electron-electron interactions are involved, the applicability of our FRG procedure is limited to 2D diffusive conductors. The generalized FRG equation that takes into account interaction constant λ in the Cooper channel of the N conductor is given by Eq. (5.8). We derive this equation and analyze its solution in Sec. V analytically in two limiting cases of weak interaction of arbitrary sign and of strong repulsion. We also provide the results of numerical solution of Eq. (5.8) in the intermediate region of moderate repulsion. The main feature of the interaction effect in 2D is that it leads to the infrared-growing corrections of the order of $\lambda\ln(L/d)$, which should be summed up nonperturbatively for the system of sufficiently large size L, for any value of the ratio G_T/G_D. This is in contrast with the 1D case (as treated in Ref. 17 for the case of the fully transparent interface, $G_T^{-1}=0$), where the interaction correction to the resistance was found to be small, of the order of λ itself.

The physical consequences of Cooper repulsion in a 2D proximity system depend on the relation between λ and the ratio $G_T/4\pi g$. For clarity, we assumed that the interaction constant had reached Finkelstein's fixed point $\lambda=1/2\pi\sqrt{g}$. Thus, strong repulsion corresponds to a relatively weak tunneling conductance $G_T\ll 2\sqrt{g}$ and vice versa. It is convenient to characterize N-I-S transport in terms of an effective interface resistance $R_{T,\rm eff}$, so that the total resistance is equal to $R_D+R_{T,\rm eff}$. If $G_T\ll 2\sqrt{g}$, then $R_{T,\rm eff}\approx(4\sqrt{g}/G_T)R_T\gg R_T$. This asymptotic result is valid at $t\geqslant G_T/\sqrt{g}$. At longer length scales, such that $\ln(L/d)\geqslant\pi\sqrt{g}$, Cooper-channel correlations are irrelevant and the form of the proximity action coincides with that of an N-I-N structure, up to the replacements of charge quantum and tunneling resis-

tance: $e\to 2e$ and $R_T\to R_{T,\mathrm{eff}}$. As a particular example of this property, in Sec. V D we calculated the N-I-S noise intensity. In the opposite case, $G_T\gg 2\sqrt{g}$, the evolution of $R_{T,\mathrm{eff}}$ with the growth of t is rather unexpected (cf. Fig. 11): first it decreases with t, reaches a minimum value of the order of R_T at $t\sim(G_T/\sqrt{g})^{1/4}$, and then grows up to the asymptotic value $0.6\hbar/e^2\sqrt{g}$ at $t\gg G_T/\sqrt{g}$. Nonmonotonous behavior with a maximum of relative height about 30% is demonstrated by the noise power as well; cf. Sec. V D.

At finite temperature, voltage, or magnetic field Cooperon coherence is destroyed at the time of the order of $\hbar/\Omega_*$, where $\Omega_*=\max(T,eV,eDH/c)$. We calculated the Andreev conductance and shot noise power in the presence of these phase-breaking effects in Sec. VI B for a noninteracting normal conductor. The role of phase-breaking effects in the presence of repulsion in the normal conductor is discussed in Sec. VI C. In the case of a highly transparent interface, $G_T\gg 2\sqrt{g}$, and at $R_D\gg R_T$, an unusual ''finite-bias'' maximum of the Andreev conductance $G_A(\Omega_*)$ is predicted (cf. Fig. 17), which is a consequence of the nonmonotonous behavior of $R_{T,\mathrm{eff}}(t)$ mentioned above. Contrary to the well-known[35,17] finite-bias anomaly at $(T,eV)\sim E_{\mathrm{Th}}$ in the noninteracting case, this new anomaly is expected at a much larger value of Ω_*/E_{Th}. Moreover, it should be seen as a function of magnetic field as well. In simple terms the origin of this new effect can be understood as follows: repulsion in the normal metal produces a superconductive ''gap function'' in the normal conductor, Δ_N, with negative (compared to Δ_S in a superconductor) sign. Due to its opposite sign, Δ_N decreases the conductance of the structure; therefore any decoherence that reduces Δ_N leads to the increase of the conductance.

We did not consider in this paper the weak localization (WL) effect and the Coulomb zero-bias anomaly. The reason to neglect them, as explained in the Introduction, is that relative magnitudes of these effects scale as $g^{-1}|\ln\Omega|$. However, both of these effects have a high-frequency cutoff at the inverse elastic scattering time $1/\tau$, and their contributions to the tunneling and diffusive conductances from the energy scales $\omega_d<\Omega<1/\tau$ are not necessarily small. Since logarithmic corrections to the proximity action we have studied are coming from much lower-energy scales $\Omega\leqslant\omega_d$, these effects can be considered separately: high-frequency fluctuations can be accounted via the replacement of the bare conductances G_T and g by their values corrected by the WL and ZBA effects at the energy scales $\omega_d<\Omega<1/\tau$, provided that the renormalized value of g is still large.

In this paper we consider the low-frequency case $\omega\ll E_{\mathrm{Th}}$ only. This limitation is due to technical complications: at higher frequencies the effects of dynamic screening should be taken into account, which makes the expression for the proximity action much more involved. However, it is possible to show that the results obtained for the Andreev conductance are still valid for frequencies up to a much higher-frequency scale $\omega_{\max}$ [defined after Eq. (4.5)] at which the electroneutrality of the system sets in. Experimentally, N-S noise in the presence of high-frequency radiation ($\omega\gg E_{\mathrm{Th}}$) was studied in Ref. 38. We leave theoretical consideration of this problem for the future.

ACKNOWLEDGMENTS

We are grateful to Ya.M. Blanter, G.B. Lesovik, and Yu. V. Nazarov for useful discussions. This research was supported by NSF Grant No. DMR-9812340 (A.I.L.), NWO-Russia Collaboration grant, Swiss NSF-Russia Collaboration grant, RFBR Grant No. 98-02-16252, and the Russian Ministry of Science within the project ''Mesoscopic electron systems for quantum computing'' (M.V.F. and M.A.S.).

APPENDIX A: CONTRACTION RULES

The contraction rule for averaging over W is given by[1]

$$\langle \mathrm{Tr}AW\cdot \mathrm{Tr}BW\rangle=\frac{1}{2\pi\nu}\int\frac{d\mathbf{q}d\epsilon_1 d\epsilon_2}{(2\pi)^4}X(\mathbf{q},\epsilon_1,\epsilon_2), \tag{A1}$$

where

$$X=\frac{\mathrm{tr}[A_{12}\Lambda_2 B_{21}\Lambda_1+A_{12}(\Lambda_0)_2 B_{21}(\Lambda_0)_1-A_{12}\tau_z B_{21}\tau_z-A_{12}B_{21}][Dq^2+i(\epsilon_1-\epsilon_2)(\Lambda_0)_1]}{(Dq^2)^2+(\epsilon_1-\epsilon_2)^2}$$
$$+\frac{\mathrm{tr}[A_{12}\Lambda_2 B_{21}\Lambda_1-A_{12}(\Lambda_0)_2 B_{21}(\Lambda_0)_1+A_{12}\tau_z B_{21}\tau_z-A_{12}B_{21}][Dq^2+i(\epsilon_1+\epsilon_2)(\Lambda_0)_1]}{(Dq^2)^2+(\epsilon_1+\epsilon_2)^2}. \tag{A2}$$

Here $A_{12}\equiv A(\mathbf{q},\epsilon_1,\epsilon_2)$, $B_{21}\equiv B(-\mathbf{q},\epsilon_2,\epsilon_1)$, $\Lambda_m\equiv\Lambda(\epsilon_m)$, and $(\Lambda_0)_m\equiv\Lambda_0(\epsilon_m)$. The first (second) line of Eq. (A2) corresponds to diffuson (Cooperon) pairing.

In the zero-energy limit $Dq^2\gg\epsilon_1,\epsilon_2$, this expression can be simplified as

$$\langle \mathrm{Tr}AW\cdot \mathrm{Tr}BW\rangle=\frac{2}{\pi g}\int\frac{d\mathbf{q}d\epsilon_1 d\epsilon_2}{(2\pi)^4}\frac{\mathrm{tr}(A_{12}\Lambda_2 B_{21}\Lambda_1-A_{12}B_{21})}{q^2}. \tag{A3}$$

APPENDIX B: CONTRIBUTION OF A SINGLE TERM FROM THE MULTICHARGE ACTION TO THE CONDUCTANCE AND NOISE

Here we calculate the quantity which describes the contribution of a single term from the action (3.15) to the dc conductance of the system in the zero-energy limit ($\Omega_* \ll E_{\rm Th}$):

$$\frac{\delta}{\delta\varphi_2}\mathrm{Tr}_K(e^{i\vec{\varphi}}\Lambda_0 e^{-i\vec{\varphi}}\Lambda_0)^n\big|_{\varphi_2=0}, \tag{B1}$$

with φ_1 obeying the Josephson relation $\dot{\varphi}_1=2eV$. The derivative can act either on $e^{i\vec{\varphi}}$ or on $e^{-i\vec{\varphi}}$ so that Eq. (B1) reduces to

$$in\int_{-\infty}^{\infty}\frac{d\epsilon}{2\pi}\mathrm{tr}_K\sigma_x[M^n(V)-M^n(-V)], \tag{B2}$$

where M is diagonal in the energy space matrix,

$$M_{\epsilon\epsilon}(V)=\Lambda_0(\epsilon_+)\Lambda_0(\epsilon_-)=\begin{pmatrix}1 & 2[F(\epsilon_-)-F(\epsilon_+)]\\ 0 & 1\end{pmatrix}_K, \tag{B3}$$

and $\epsilon_\pm=\epsilon\pm eV$. Calculating M^n, integrating over ϵ, and tracing with σ_x one finds that both terms in Eq. (B2) yield the same contributions, and

$$\frac{\delta}{\delta\varphi_2}\mathrm{Tr}_K(e^{i\vec{\varphi}}\Lambda_0 e^{-i\vec{\varphi}}\Lambda_0)^n\big|_{\varphi_2=0}=\frac{8i}{\pi}n^2eV. \tag{B4}$$

In a similar way one can obtain

$$\frac{\delta}{\delta\varphi_2}\mathrm{Tr}_K(e^{i\vec{\varphi}/2}\Lambda_0 e^{-i\vec{\varphi}/2}\Lambda_0)^n\big|_{\varphi_2=0}=\frac{2i}{\pi}n^2eV. \tag{B5}$$

Now we turn to another expression emerging in calculation of the current-current correlator from the action (3.1):

$$L_n(t,t';V)=\frac{\delta^2}{\delta\varphi_2(t)\,\delta\varphi_2(t')}\mathrm{Tr}_K(e^{i\vec{\varphi}}\Lambda_0 e^{-i\vec{\varphi}}\Lambda_0)^n\big|_{\varphi_2=0}. \tag{B6}$$

Here there are several possibilities depending on where the derivatives act on. First of all we note that they cannot act on the same exponent $e^{i\vec{\varphi}}$ (or $e^{-i\vec{\varphi}}$). Indeed, in this case Eq. (B6) would reduce to $\mathrm{Tr}M^n(V)\propto\mathrm{Tr}\mathbb{1}$ that would give zero according to the rules of the Keldysh σ model.[21] Therefore there are four different contributions (coinciding time indices t,t' are omitted):

$$L_n(V)=L_n^a(V)+L_n^a(-V)+L_n^b(V)+L_n^b(-V). \tag{B7}$$

Performing a Fourier transformation to the frequency domain one obtains

$$L_n^a(\omega;V)=n\sum_{\substack{p,q\geqslant 0\\ p+q=n-1}}\int_{-\infty}^{\infty}\frac{d\epsilon}{2\pi}\times\mathrm{tr}_K\{\Lambda_0 M^p(-V)\sigma_x\}_{\epsilon+\omega+2eV}\{\Lambda_0 M^q(V)\sigma_x\}_\epsilon,$$

$$L_n^b(\omega;V)=-n\sum_{\substack{r,s\geqslant 0\\ r+s=n-2}}\int_{-\infty}^{\infty}\frac{d\epsilon}{2\pi}\mathrm{tr}_K\Lambda_0(\epsilon+\omega+2eV)\times\{\Lambda_0 M^r(V)\sigma_x\}_{\epsilon+\omega}\Lambda_0(\epsilon+2eV)\times\{\Lambda_0 M^s(V)\sigma_x\}_\epsilon.$$

Evaluating matrix powers and computing traces we obtain

$$L_n^a(\omega;V)=4n\sum_{\substack{p,q\geqslant 0\\ p+q=n-1}}\int_{-\infty}^{\infty}[(p+1)F(\epsilon+\omega+2eV)-pF(\epsilon+\omega)][(q+1)F(\epsilon)-qF(\epsilon+2eV)]\frac{d\epsilon}{2\pi},$$

$$L_n^b(\omega;V)=-4n\sum_{\substack{r,s\geqslant 0\\ r+s=n-2}}(r+1)(s+1)\times\int_{-\infty}^{\infty}[F(\epsilon+\omega)-F(\epsilon+\omega+2eV)]\times[F(\epsilon)-F(\epsilon+2eV)]\frac{d\epsilon}{2\pi}.$$

Now integrating over energy with the help of Eq. (4.7), we arrive at

$$L_n^a(\omega;V)=\frac{4n}{\pi}\sum_{\substack{p,q\geqslant 0\\ p+q=n-1}}\{2(p+1)q\Psi(\omega)-pq\Psi(\omega-2eV)-(p+1)(q+1)\Psi(\omega+2eV)\},$$

$$L_n^b(\omega;V)=\frac{4n}{\pi}\sum_{\substack{r,s\geqslant 0\\ r+s=n-2}}(r+1)(s+1)[2\Psi(\omega)-\Psi(\omega-2eV)-\Psi(\omega+2eV)].$$

Evaluating the sums with the help of

$$\sum_{\substack{p,q\geqslant 0\\ p+q=n-1}}pq=\binom{n}{3},$$

$$\sum_{\substack{p,q\geqslant 0\\ p+q=n-1}}(p+1)q=\sum_{\substack{r,s\geqslant 0\\ r+s=n-2}}(r+1)(s+1)=\binom{n+1}{3},$$

$$\sum_{\substack{p,q\geqslant 0\\ p+q=n-1}}(p+1)(q+1)=\binom{n+2}{3},$$

we get

$$L_n^a(\omega;V)+L_n^b(\omega;V)=\frac{2n^2}{3\pi}\{4(n^2-1)\Psi(\omega) -(n-1)(2n-1)\Psi(\omega-2eV) -(n+1)(2n+1)\Psi(\omega+2eV)\}. \tag{B8}$$

Finally, substituting Eq. (B8) into Eq. (B7), we obtain

$$\frac{\delta^2}{\delta\varphi_2(\omega)\delta\varphi_2(-\omega)}\mathrm{Tr}_K(e^{i\vec{\varphi}}\Lambda_0 e^{-i\vec{\varphi}}\Lambda_0)^n|_{\varphi_2=0} =-\frac{4n^2}{3\pi}\{(2n^2+1)[\Psi(\omega-2eV)+\Psi(\omega+2eV)] -4(n^2-1)\Psi(\omega)\}. \tag{B9}$$

Analogously,

$$\frac{\delta^2}{\delta\varphi_2(\omega)\delta\varphi_2(-\omega)}\mathrm{Tr}_K(e^{i\vec{\varphi}/2}\Lambda_0 e^{-i\vec{\varphi}/2}\Lambda_0)^n|_{\varphi_2=0} =-\frac{n^2}{3\pi}\{(2n^2+1)[\Psi(\omega-eV)+\Psi(\omega+eV)] -4(n^2-1)\Psi(\omega)\}. \tag{B10}$$

APPENDIX C: SOLUTION OF THE USADEL EQUATION IN THE FIRST ORDER OVER λ

We will generalize here the method used in Ref. 17 for the calculation of G_A in the presence of an interaction. Since we consider general case of an arbitrary interface transparency, the first step will be to find the interaction-induced correction to the ''spectral angle'' $\theta_E(r)$ that parametrizes[5,17] the retarded semiclassical Green function in the N conductor,

$$\hat{G}^R(E)=\begin{pmatrix}\cos\theta & ie^{i\varphi}\sin\theta\\ -ie^{-i\varphi}\sin\theta & -\cos\theta\end{pmatrix}, \tag{C1}$$

where the proximity angle θ and the order parameter phase φ depend on the energy E and the space coordinate $\mathbf{r}$. In N-S systems with a single superconductive terminal physical quantities do not depend on the phase on it, $\varphi(0)$, so below we put $\varphi(0)=-\pi/2$. In general, when interaction in the N conductor is present, normal current flowing through the N-S structure induces a supercurrent $\mathbf{j}_s\propto\nabla\varphi$, so that the phase $\varphi(\mathbf{r})$ acquires some nontrivial distribution. However, this effect appears in the second order of expansion over Cooper interaction constant λ_d. Below we solve the Usadel equation within the first order over λ_d, neglecting, therefore, the effects of supercurrent.

1. Spectral angle

The Usadel equation for the spectral angle $\theta_E(r)$ has the form

$$D\nabla^2\theta_E+2iE\sin\theta_E+2\Delta\cos\theta_E=0, \tag{C2}$$

where the self-consistency equation for the order parameter reads

$$\Delta(r)=-\lambda_d\int_0^\infty dE\tanh\frac{E}{2T}\mathrm{Im}\sin\theta_E, \tag{C3}$$

and the interaction constant λ_d at the energy scale ω_d is defined in Eq. (5.10). We assume that the main contribution to Δ comes from relatively high E, where $\theta_E(r)$ is small everywhere. Hence, Eq. (C2) can be linearized, and the last term can be neglected once we are interested in the first-order corrections over λ_d to G_A. The result is

$$\theta_E(r)=A(E)K_0[(1-i)r/L_E], \tag{C4}$$

where $L_E=\sqrt{D/E}$, and A is determined by the boundary condition

$$g\frac{d\theta_E(r)}{dr}|_{r=d}=-\frac{G_T}{2\pi d}\cos\theta_E(r=d). \tag{C5}$$

The solution for $A(E)$ is conveniently expressed in terms of the function $\Theta(t)$ defined in Eq. (4.15): $A(E)=\Theta(t_E)/\ln(L_E/d)$, where $t_E=a\ln(\omega_d/E)$. Substituting $\theta_E(r)$ into Eq. (C3), and using the identity $\int_0^\infty xK_0(x)dx=1$ and logarithmic slowness of $A(t_E)$ as a function of E, we find for $\Delta(r)$

$$\Delta(r)=-\frac{\lambda_d D}{r^2}\frac{\Theta(2a\ln(r/d))}{\ln(r/d)}. \tag{C6}$$

The next step is to solve for $\theta_{E=0}(r)$ with $\Delta(r)$ taken into account:

$$\frac{d^2\theta}{dr^2}+\frac{1}{r}\frac{d\theta}{dr}=\frac{2\lambda_d}{r^2}\frac{\Theta(2a\ln(r/d))}{\ln(r/d)}\cos\theta. \tag{C7}$$

In terms of the variable $\xi=\ln(r/d)$, this equation reduces to

$$\frac{d^2\theta}{d\xi^2}=2\lambda_d\frac{\Theta(2a\xi)}{\xi}\cos\theta, \tag{C8}$$

with the boundary conditions $\theta(\xi_L)=0$ and $\theta_\xi(0)=-2a\cos\theta(0)$, where $\xi_L=\ln(L/d)$. To the lowest order in λ_d one obtains

$$\theta(\xi)=\Bigg\{\Theta(2a\xi_L) -2\lambda_d\xi_L\int_0^{\xi_L}\frac{1+2a\eta\sin\Theta(2a\xi_L)}{1+2a\xi_L\sin\Theta(2a\xi_L)}\frac{\Theta(2a\eta)}{\eta} \times\cos\left[\Theta(2a\xi_L)\left(1-\frac{\eta}{\xi_L}\right)\right]d\eta\Bigg\}\left(1-\frac{\xi}{\xi_L}\right)+2\lambda_d \times\int_\xi^{\xi_L}(\eta-\xi)\frac{\Theta(2a\eta)}{\eta}\cos\left[\Theta(2a\xi_L)\left(1-\frac{\eta}{\xi_L}\right)\right]d\eta. \tag{C9}$$

Taking into account that $2a\xi_L = a\zeta \equiv t$, and evaluating expression (C9) at $\xi = 0$, we obtain the spectral angle near the interface, $\theta_d \equiv \theta(\xi = 0)$:

$$\theta_d = \Theta(t) - \frac{\lambda_d \zeta}{1 + t \sin\Theta(t)} \times \int_0^1 \frac{\Theta(xt)}{x}(1-x)\cos[\Theta(t)(1-x)]dx. \quad \text{(C10)}$$

2. Distribution function and G_A

To find G_A we use the kinetic equation in the form developed in Ref. 17. The current density near the N reservoir (at $r = L$) is

$$j_N(R) = g \int dE \left.\frac{df_1(E,r)}{dr}\right|_{r=L}, \quad \text{(C11)}$$

where $f_1(E,r)$ is the anomalous (branch imbalance) distribution function, defined after Eq. (2.2). Note that Eq. (C11) is valid only at the boundary with the normal lead where $\theta = 0$ (otherwise it should be modified by the presence of the supercurrent $\mathbf{j}_s \propto \lambda_d$). The function $f_1(E,r)$ obeys the equation

$$\nabla D(r,E) \nabla f_1(E,r) = 2\Delta(r)\sin\theta(E,r) f_1(E,r). \quad \text{(C12)}$$

We will assume that the normal reservoir is biased by the voltage V, so that the whole distribution function is shifted: $F(E,L) = \tanh(E + eV\tau_z)/2T \approx \tanh(E/2T) + \tau_z (eV/2T)\cosh^{-2}(E/2T)$ and

$$f_1(E,L) = eVc(E) = \frac{eV}{2T}\cosh^{-2}\frac{E}{2T}. \quad \text{(C13)}$$

At $T \to 0$ it is enough to consider Eq. (C12) at zero energy, where $D(0,r) = D$, and the solution for $\theta(0,r)$ is given by $\theta(0,r) = \theta_d \ln(L/r)/\ln(L/d)$, with θ_d given by Eq. (C10). Then equation for $f_1(r)$ reduces to

$$\frac{d^2 f_1}{d\xi^2} = -2\lambda_d \frac{\Theta(2a\xi)}{\xi}\sin\left[\theta_d\left(1 - \frac{\xi}{\xi_L}\right)\right] f_1. \quad \text{(C14)}$$

We seek the solution of Eq. (C14) in the form $f_1(\xi) = f_1^{(0)}(\xi) + \lambda_d f_1^{(1)}(\xi)$, where

$$f_1^{(0)}(\xi) = eVc(E)\left[\frac{\xi}{\xi_L} + v_d\left(1 - \frac{\xi}{\xi_L}\right)\right]. \quad \text{(C15)}$$

The function $c(E)$ was defined in Eq. (C13), and the parameter $v_d = V_d/V$ should be determined from the boundary condition to the Usadel equation:

$$\left.\frac{\partial f_1}{\partial \xi}\right|_{\xi=0} = 2a f_1 \sin\theta_d, \quad \text{(C16)}$$

which gives $v_d = 1/(1 + t\sin\theta_d)$.

The general solution of Eq. (C14) for the function $f_1^{(1)}$ can be written as

$$f_1^{(1)}(\xi) = \int_0^\xi (\xi - \eta) y(\eta) d\eta + C_1 \xi + C_0, \quad \text{(C17)}$$

where $y(\xi) = -2\lambda_d(\Theta(a\xi)/\xi)\sin[\Theta(t)(1-\xi/\xi_L)] f_1^{(0)}(\xi)$. Using Eq. (C16) and the condition $f_1^{(1)}(\xi_L) = 0$, we find the constants C_0 and C_1, and obtain

$$\left.\frac{\partial f_1^{(1)}}{\partial \xi}\right|_{\xi_L} = \frac{1}{\xi_L}\int_0^{\xi_L} \frac{\xi_L + \eta t \sin\Theta(t)}{1 + t\sin\Theta(t)} y(\eta) d\eta. \quad \text{(C18)}$$

Calculating the total current as $I_N = 2\pi L j_N(L)$ where $j_N(L)$ is determined by Eq. (C11) and introducing $x = \eta/\xi_L$, we obtain for the Andreev conductance

$$\frac{G_A}{G_D} = \frac{t\sin\theta_d}{1 + t\sin\theta_d} - \lambda_d \zeta \int_0^1 \frac{[1 + xt\sin\Theta(t)]^2}{[1 + t\sin\Theta(t)]^2}\frac{\Theta(xt)}{x} \times \sin[\Theta(t)(1-x)]dx, \quad \text{(C19)}$$

with θ_d defined in Eq. (C10).

Equation (C19) is an exact answer in the first order over λ_d (in this approximation the supercurrent does not yet mix equations for f_1 and f). In the $t \to \infty$ limit of Eq. (C19), i.e., at $G_T \gg G_D$, the interaction-induced correction is

$$\frac{G_A}{G_D} = 1 - 2\frac{\pi - 2}{\pi}\lambda_d \ln\frac{L}{d} \quad \text{(C20)}$$

and grows with the space scale, in contrast with the results of Ref. 17 obtained for the 1D geometry.

[1] M.V. Feigel'man, A.I. Larkin, and M.A. Skvortsov, Phys. Rev. B **61**, 12 361 (2000).

[2] A.F. Andreev, Zh. Éksp. Teor. Fiz. **46**, 1823 (1964) [Sov. Phys. JETP **19**, 1228 (1964)].

[3] A.F. Volkov, A.V. Zaitsev, and T.M. Klapwijk, Physica C **210**, 21 (1993).

[4] Yu.V. Nazarov, Phys. Rev. Lett. **73**, 134 (1994).

[5] Yu.V. Nazarov, Phys. Rev. Lett. **73**, 1420 (1994).

[6] C.W.J. Beenakker, Rev. Mod. Phys. **69**, 731 (1997).

[7] B. Pannetier and H. Courtois, J. Low Temp. Phys. **118**, 599 (2000).

[8] B.L. Altshuler and A.G. Aronov, in *Electron-Electron Interactions in Disordered Conductors*, edited by A.J. Efros and M. Pollack (North-Holland, Amsterdam, 1985).

[9] E. Abrahams, P.W. Anderson, D.C. Licciardello, and T.V. Ramakrishnan, Phys. Rev. Lett. **42**, 673 (1979).

[10] L.P. Gorkov, A.I. Larkin, and D.E. Khmelnitsky, Pis'ma Zh. Éksp. Teor. Fiz. **30**, 248 (1979) [JETP Lett. **30**, 228 (1979)].

[11] B.L. Altshuler, A.G. Aronov, and P.A. Lee, Phys. Rev. Lett. **44**, 1288 (1980).
[12] S. Maekawa and H. Fukuyama, J. Phys. Soc. Jpn. **51**, 1380 (1982).
[13] H. Takagi and Y. Kuroda, Solid State Commun. **41**, 643 (1982).
[14] A.M. Finkelstein, Pis'ma Zh. Éksp. Teor. Fiz. **45**, 37 (1987) [JETP Lett. **45**, 46 (1987)].
[15] A.M. Finkelstein, *Electron Liquid in Disordered Conductors*, Vol. 14 of *Soviet Scientific Reviews*, edited by I.M. Khalatnikov (Harwood Academic, London, 1990).
[16] A.M. Finkelstein, Physica B **197**, 636 (1994).
[17] T.H. Stoof and Yu.V. Nazarov, Phys. Rev. B **53**, 14 496 (1996).
[18] M.J.M. de Jong and C.W.J. Beenakker, Phys. Rev. B **49**, 16 070 (1994).
[19] G.B. Lesovik, T. Martin, and J. Torres, Phys. Rev. B **60**, 11 935 (1999).
[20] Ya.M. Blanter and M. Büttiker, Phys. Rep. **336**, 1 (2000).
[21] A. Kamenev and A. Andreev, Phys. Rev. B **60**, 2218 (1999).
[22] C.W.J. Beenakker, B. Rejaei, and J.A. Melsen, Phys. Rev. Lett. **72**, 2470 (1994).
[23] A.I. Larkin and Yu.N. Ovchinnikov, in *Nonequilibrium Superconductivity*, edited by D.N. Langenberg and A.I. Larkin (Elsevier, New York, 1986).
[24] J. Rammer and H. Smith, Rev. Mod. Phys. **58**, 323 (1986).
[25] K. Usadel, Phys. Rev. Lett. **25**, 507 (1970).
[26] O.N. Dorokhov, Solid State Commun. **51**, 381 (1984).
[27] M.V. Feigel'man, A.I. Larkin, and M.A. Skvortsov, cond-mat/0010402, Phys. Rev. Lett. (to be published).
[28] C.W.J. Beenakker and M. Büttiker, Phys. Rev. B **46**, 1889 (1992).
[29] K.E. Nagaev, Phys. Lett. A **169**, 103 (1992).
[30] L.S. Levitov and G.B. Lesovik, Pis'ma Zh. Éksp. Teor. Phys. **58**, 225 (1993) [JETP Lett. **58**, 230 (1993)].
[31] H. Lee, L.S. Levitov, and A.Yu. Yakovets, Phys. Rev. B **51**, 4079 (1995).
[32] C.W.J. Beenakker, Phys. Rev. B **46**, 12 841 (1992).
[33] B.A. Muzykantskii and D.E. Khmelnitskii, Phys. Rev. B **50**, 3982 (1994).
[34] Performing averaging over the shadowed diffuson and Cooperons with the help of Eq. (A2), one obtains an expression similar to Eq. (5.3). However, now the trace contains the difference $\mathcal{M}_3 - \mathcal{M}_1$ [cf. Eq. (5.4)], which vanishes according to the theorem proved after Eq. (5.4).
[35] S.N. Artemenko, A.F. Volkov, and A.V. Zaitsev, Solid State Commun. **30**, 771 (1995).
[36] B.L. Altshuler, D.E. Khmelnitskii, A.I. Larkin, and P.A. Lee, Phys. Rev. B **22**, 5142 (1980).
[37] This result is in agreement with experimental data on the *dc* current noise in S-N junction presented in Ref. 38. In that experiment the case $G_T \gg G_N$ was realized, and behavior of the noise power was found to be the same both at small and large eV compared to E_{Th}.
[38] A.A. Kozhevnikov, R.J. Schoelkopf, and D.E. Prober, Phys. Rev. Lett. **84**, 3398 (2000).